siam

10th Annual Meeting of the Bulgarian Section of SIAM
December 21-22, 2015
Sofia

BGSIAM'15

PROCEEDINGS

HOSTED BY THE INSTITUTE OF MATHEMATICS AND INFORMATICS
BULGARIAN ACADEMY OF SCIENCES

10th Annual Meeting of the Bulgarian Section of SIAM
December 21-22, 2015, Sofia

BGSIAM'15 Proceedings

ISSN: 1313-3357

Printed in Sofia, Bulgaria

PREFACE

The Bulgarian Section of SIAM (BGSIAM) was formed in 2007 with the purpose to promote and support the application of mathematics to science, engineering and technology in Republic of Bulgaria. The goals of BGSIAM follow the general goals of SIAM:

- To advance the application of mathematics and computational science to engineering, industry, science, and society;
- To promote research that will lead to effective new mathematical and computational methods and techniques for science, engineering, industry, and society;
- To provide media for the exchange of information and ideas among mathematicians, engineers, and scientists.

During BGSIAM'15 conference a wide range of problems concerning recent achievements in the field of industrial and applied mathematics will be presented and discussed. The meeting provides a forum for exchange of ideas between scientists, who develop and study mathematical methods and algorithms, and researchers, who apply them for solving real life problems. The conference support provided by SIAM is highly appreciated.

The strongest research groups in Bulgaria in the field of industrial and applied mathematics, advanced computing, mathematical modelling and applications will be presented at the meeting according to the accepted extended abstracts. Many of the participants are young scientists and PhD students.

LIST OF INVITED LECTURES:

- Tzanio Kolev, Lawrence Livermore National Laboratory, USA
  Scalable High-Order Finite Elements for Compressible Hydrodynamics
- Johannes Kraus, Universitat Duisburg-Essen, Germany
  Optimal Multigrid Methods for H(div)-Conforming Discontinuous Galerkin Discretizations of the Brinkman Problem
- Maya Neytcheva, Uppsala University, Sweden
  Efficient Numerical Methods for Time Evolution Processes, Described by Integro-Differential Equations
- Vladimir Veliov, Vienna University of Technology, Austria
  On the Method of Kantorovich for Non-Smooth Generalized Equations

The present volume contains extended abstracts of the presentations (Part A) and list of participants (Part B).

Krassimir Georgiev
Chair of BGSIAM Section

Michail Todorov
Vice-Chair of BGSIAM Section

Ivan Georgiev
Secretary of BGSIAM Section

Sofia, December 2015

Table of Contents

Part A
Extended abstracts[1]

[1] Arranged alphabetically according to the family name of the first author.

On Efficient Monte Carlo and quasi-Monte Carlo Preconditioners and Hybrid Methods for Linear Algebra

Vassil Alexandrov, O. Esquivel-Flores, Todor Gurov, Aneta Karaivanova

An enhanced version of a stochastic SParse Approximate Inverse (SPAI) preconditioner for general matrices is presented in this paper. These are Monte Carlo and quasi-Monte Carlo preconditioners based on Markov Chain Monte Carlo (MCMC) methods and quasi-Monte Carlo methods respectively that compute a rough approximate matrix inverse first, which can further be optimized by an iterative filter process and a parallel refinement, to enhance the accuracy of the inverse and the preconditioner respectively. The above Monte Carlo and quasi-Monte Carlo preconditioners are further used to solve systems of linear algebraic equations thus delivering hybrid stochastic/deterministic algorithms. The advantage of the proposed approach is that the sparse Monte Carlo (quasi-Monte Carlo) matrix inversion has a computational complexity linear of the size of the matrix, it is inherently parallel and thus can be obtained very efficiently for large matrices and can be used also as an efficient preconditioner while solving systems of linear algebraic equations. Computational experiments on the Monte Carlo preconditioners and the hybrid algorithms using BiCGSTAB and GMRES as SLAEs solvers are presented and the results are compared to those of MSPAI (parallel and optimized version of the deterministic SPAI) and combined MSPAI and BiCGSTAB and GMRES approaches to solve SLAEs. Some comparison between Monte Carlo and quasi-Monte Carlo approach is also made. The computational experiments are carried out on classes of matrices from the matrix market and show the efficiency of the proposed approach.

Acknowledgments: This work was supported by the National Science Fund of Bulgaria under Grant DFNI-I02/8.

Mathematical Model for a Pneumatic Force Actuator System

Andrey Andreev, Hristo Hristov, Georgi Iliev, Milena Racheva

This paper deals with a mathematical model of pneumatic actuator control. Namely, we consider cylinder tubes that connect valves with actuators. Our aim is to develop a detailed mathematical model for online control applications.
It is well-known that only through practice or relevant real measurements could say whether a model has a practical value. On the other hand, it is necessary to take into account the important factor: is the model computable, and what is more – computable in an easy way? Very often the so-called "'exact solution"' of the model differential equation is difficult and even impossible to implement in engineering practice. Here, we propose an adequate presentation of a pneumatic force system for calculation of the mass flw at the point $x = L_z$.
It is well-known (see, e.g. [1, 2]) that the basic equations governing the flow in a circular pneumatic line are written as:

$$\begin{aligned} \frac{\partial \mathcal{P}}{\partial x} &= -R\, v - \rho\, \frac{\partial v}{\partial t} \\ \frac{\partial v}{\partial x} &= -\frac{1}{\rho c^2}\, \frac{\partial \mathcal{P}}{\partial t}, \end{aligned} \tag{1}$$

where

- $\mathcal{P}$ is the pressure along the tube;
- v is the velocity;
- ρ is the air dencity;
- c denotes the sound speed.

It is not difficult to transform the main system (1) as one equation for the mass flow m through the tube:

$$\frac{\partial^2 m_t}{\partial t^2} - c^2 \frac{\partial^2 m_t}{\partial x^2} + \frac{R}{\rho}\, \frac{\partial m_t}{\partial t} = 0. \tag{2}$$

Knowing the input mass flow $m_t(0,t) = f(t)$, we consider the equation (2) with homogeneous initial conditions.
For solving the hyperbolic equation (2) the method of Laplace transform is adopted. A distinctive feature of the proposed approach is its applicability for a variety of engineering problems.
The mass flow at the outlet of the tube (i.e. $x = L_t$ and $t > \dfrac{L_t}{c}$) is:

$$m_t = \frac{R^2}{8c\rho^2}\ exp\left[\frac{R}{2\rho}\left(t - 2\frac{L_t}{c}\right)\right]\ f\left(t - \frac{L_t}{c}\right).$$

The proposed model is sufficiently simple, such that is can be used online in control applications.
Finally, the model was tested using three different values for the parameter L_z and that allowed the measurement of the actuator force output. The experimental results were compared with the results obtained by numerical model simulation.

References

[1] Andersen, B.: The Analysis and Desighn of Pneumatic Systems. New York, (John Wiley & Sons, Inc. 1967.s

[2] Elmadbouly, E.E., Abdulsadek, N.M.: Modeling, simulation and sensitivity analysis of a straight pneumatic pipeline, Energy Conservation and Management, Vol. 35, No 1, 66-77 (1994).

[3] Jordan, D.W. and Smith, P.: Mathematical Techniques. 4th edition, (Oxford 2008).

On the Security Issues in High Performance Computing

Emanouil Atanassov, Aneta Karaivanova, Todor Gurov

In this paper we investigate security issues arising in High Performance Computing both from theoretical and practical point of view, having in mind the recently acquired state of the art HPC system at Institute of Information and Communication Technologies - Bulgarian Academy of Sciences (IICT-BAS), which entered the Top500 list of supercomputers at the 332nd place in June 2015, with the aim to open the system to outside use with acceptable overall level of security.

Because of the high cost and the unique features of High Performance Computing facilities, which even make them "sensitive" infrastructure from military and political point of view, it is important to investigate the various security issues and treats that arise from the potential opening of the system to a wide community of users.

In this work we do not touch upon the questions of physical security and we also do not consider of the security of networking that are handled outside of our HPC facility, at the level of the National Research and Educational Network. We mostly concentrate on the deployment options and measures that are internal to the data centre and we also compare them with facilities that operate under more open access models, like Grids or public clouds like Amazon Web Services.

First of all we consider the security issues arising from the needs for data transfer and then we proceed with some specifics related to the computational environment.

Most of the HPC facilities that are of national importance are presented to the users as a rather closed environment with limited options of entering and data transfer. In this way the computing capabilities of the HPC system are made available to users at the price of limited amount of data that can be imported, processed or exported. The high price of data storage systems with substantial bandwidth and low latency leads to situations where some types of scientific applications can not be deployed and used efficiently. The leading protocol for remote data transfer used in the European e-Science is GridFTP, which provides security as well as high bandwidth, even when using non-dedicated network connectivity. However, this protocol requires high number of open ports in the firewall, which is a severe problem in practice. One solution adopted in the PRACE infrastructure is the establishment of a virtual private network, where only the participating HPC systems are interconnected, providing substantial guarantees. However, it does not address the case of need to transfer data between the national-level facility and the institutional level facilities, since such advanced networking capabilities are expensive and generally not available at the lower levels. It seems that a good practical approach would be to allow more flexible access when data is read-only and a more stringent security model if data has to be staged in the other direction.

In general, a layered approach that makes a distinction between classic HPC users with well understood and non-critical needs for data transfer, and advanced e-Science applications that have varying and demanding needs for data transfer, would benefit

the overall levels of security. By establishing a base level of data transfer access accessible to all with limited, but sufficient functionality in most cases, the HPC system should retain reasonable level of security and provide incentives to those users for which this functionality is not enough to move to higher level of applications.
The computational environment provided to users of the system is usually fairly standard, with direct access to hardware for maximum performance. In the public clouds usually some kind of virtualization is present, but in typical HPC deployments for the needs of science any intermediate layers are avoided for maximum performance. In our case there are certain user groups that do require cloud environment, which means that we will have to allocate dynamically computational resources that are to be virtualized. Ideally the local network will be partitioned so as to provide isolation between these types of resources. Nevertheless, the need for an interface to request and manage the cloud resources introduces additional complexity and possible attack vectors, which have to be mitigated. Overall it is necessary to deploy a sophisticated logging and monitoring system is necessary in order to be able to trace any kind of suspicious activity.
In our view it is of equal importance to be able to manage the overall computational and storage resource from one central access point, so that each group of users is awarded the minimal level of access that it requires for their research. Based on our experience within regional projects like SEE-GRID and HP-SEE, where IICT-BAS has been responsible for important parts of the centralized resource management and accounting, we developed an architecture and aim at the practical deployment of a resource management system that fulfils those goals. All user and administrator access to it is web-based, while all the changes in the user attributes are stored in a database back-end and are exposed from LDAP server, so that they can be used in the actual operations of the system. In such a way non-local changes that happen in european or regional level infrastructures are also incorporated after appropriate filtering, so that access is granted also to the non-local users that have been granted access from there.
In general, the operations of such a complex HPC system require a combination of tools and services that automate as many of the administrative tasks as possible, while providing sufficiently fine-grained control options. Initially tools and services that have been already tested in actual operations will be deployed in a conservative way, so that we can gradually add new functionality according to arising requirements.
Acknowledgments: This work was supported by the National Science Fund of Bulgaria under Grant DFNI-I02/8 and by EC programme HORIZON2020, Grant Agreement No: 675121, VI-SEEM project.

Resolvent Method Application for Building Special Solutions of Control Theory Problems

Aleksey Balabanov

In modern control theory there is an extensive range of application of the matrix algebraic Riccati equation (ARE)

$$A^T X + XA + P - XQX = 0. \tag{1}$$

Will not be exaggeration to say that in solving of linear quadratic Gaussian and H_∞ optimization problems a stabilizing solution of ARE plays the central role. The stabilizing solution to the algebraic Riccati Equation makes possible constructing feedback providing the stability of the closed-loop system and is the most important for practical applications.
In equation (1) matrices $A, P, Q \in R^{n\times n}$, $P = P^T \geq 0, \quad Q = Q^T \geq 0$ are defined by the applied problem content and the matrix $X \in R^{n\times n}$ is called the stabilizing solution when matrix $A_* = A - QX$ is Hurwitz.
The stabilizing solution can be found by resolvent method [1] from linear equation

$$U_2 X + U_1 = 0, U_1,\ U_2 \in R^{2n\times n}, \tag{2}$$

if and only if $rank\ U_2 = n$. Above in (2) $2n \times 2n$ real matrix $U = [U_1 \ \ U_2]$ is defined as integral

$$U = \frac{1}{2\pi j}\int_C \Theta(s)ds \tag{3}$$

from resolvent $\Theta(s) = (sI_{2n} - H)^{-1}$ of Hamilton matrix $H = \begin{bmatrix} A & -Q \\ -P & -A^T \end{bmatrix}$, where C is an anticlockwise closed contour in right half complex plane (s) with semicircle shape and diameter on imaginary axes which cover all right poles of resolvent $\Theta(s)$.
In the paper for matrix (3) was proposed a representation

$$U = \frac{1}{2}I_{2n} + HS,\ S = \sum_{k=0}^{n-1}\eta_{n-1-k}G^k,\ G = H^2, \tag{4}$$

where I_{2n} – $2n \times 2n$ identity matrix and η_m, $m = 0, 1, ..., n-1$ – values of quadratic functionals.
For matrices $\Theta(s),\ G^k,\ S,\ U$ some symmetry properties of their blocks were proved. Then, representation (4) application was discussed.
The representation (4) allows us to get a lot of profitable results while constructing stabilizing solution of ARE according to the special structure of applied optimization problem. For instance, in the paper were discussed the following problems. The problem of quadratic stabilization of a control system with colored external disturbance, given by data

$$H = \begin{bmatrix} A_{11} & A_{12} & -Q_{11} & 0 \\ 0 & A_{22} & 0 & 0 \\ -P_{11} & 0 & -A_{11}^T & 0 \\ 0 & 0 & -A_{12}^T & -A_{22}^T \end{bmatrix}, G = \begin{bmatrix} G_{11} & G_{12} & G_{13} & 0 \\ 0 & G_{22} & 0 & 0 \\ G_{31} & G_{34} & G_{11}^T & 0 \\ -G_{34}^T & 0 & G_{12}^T & G_{22}^T \end{bmatrix},$$

and the optimal quadratic tracking problem with initial data

$$H = \begin{bmatrix} A_{11} & 0 & -Q_{11} & 0 \\ 0 & A_{22} & 0 & 0 \\ -P_{11} & -P_{12} & -A_{11}^T & 0 \\ -P_{12}^T & -P_{22} & 0 & -A_{22}^T \end{bmatrix}, G = \begin{bmatrix} G_{11} & G_{12} & G_{13} & 0 \\ 0 & G_{22} & 0 & 0 \\ G_{31} & G_{32} & G_{11}^T & 0 \\ -G_{32}^T & G_{42} & G_{12}^T & G_{22}^T \end{bmatrix}.$$

Also, in the paper, the representation (4) applying is illustrated for one special linear quadratic optimization problem of discrete time system, which is related to the transport theory.

Acknowledgement: The research work presented in this paper is partially supported by the FP7 grant AComIn No. 316087, funded by the European Commission in Capacity Programme in 2012–2016.

References. [1] Barabanov, A.T. A Stabilizing Solution to the Algebraic Riccati Equation. The Resolvent Method. Journal of Computer and Systems Sciences International, Vol. 47, No. 3, 2008.

On the Use of Split-Quaternion Factorizations in Relativity and Scattering Theory

Danail S. Brezov, Clementina D. Mladenova, Ivaïlo M. Mladenov

We generalize an old result due to Piña [1] about the three-dimensional rotations to the hyperbolic case and utilize it to construct a specific factorization scheme for the isometries in $\mathbb{R}^{2,1}$. Although somewhat restrictive compared to Euler-type decompositions (cf. [2, 3]), our setting allows for gimbal lock control and decouples the dependence on the compound transformation's invariant axis and angle (rapidity), which provides convenience from both theoretical and practical point of view. In some particularly symmetric cases the solutions are given directly by the natural parametrization in one of the classical models of hyperbolic geometry. Apart from the obvious applications to 2+1 dimensional relativity, we discuss this new approach in the context of split-quaternion description of quantum-mechanical scattering.

References

[1] Piña E., *A New Parametrization of the Rotation Matrix*, Am. J. Phys. **51** (1983) 375-379.

[2] Brezov D., Mladenova C. and Mladenov I., *Vector Parameters in Classical Hyperbolic Geometry*, J. Geom. Symmetry Phys. **30** (2013) 21-50.

[3] Brezov D., Mladenova C. and Mladenov I., *A Decoupled Solution to the Generalized Euler Decomposition Problem in* $\mathbb{R}^3$ *and* $\mathbb{R}^{2,1}$, J. Geom. Symmetry Phys. **33** (2014) 47-78.

On the method of Kantorovich for non-smooth generalized equations

R. Cibulka, A. L. Dontchev, J. Preininger, T. Roubal, V. M. Veliov

In 1948, Kantorovich considered the Newton method for solving the equation $f(x) = 0$ and proved convergence by imposing conditions on the derivative $Df(x_0)$ of the function f and the residual $\|f(x_0)\|$ at the starting point x_0. These conditions can be actually checked, in contrast to the conventional approach to assume that the derivative $Df(\bar{x})$ at a (unknown) root $\bar{x}$ of the equation is invertible and then claim that if the iteration starts close enough to $\bar{x}$ then it generates a convergent to $\bar{x}$ sequence. For this reason Kantorovich's theorem can also be used for proving existence of a solution. In the Newton iteration procedure the derivative $Df(x_k)$ is calculated at every step and the rate of convergence is quadratic. In a related work, Kantorovich showed that to achieve linear convergence to a solution there is no need to calculate during iterations the derivative $Df(x_k)$ at the current point x_k – it is enough to use at each iteration the value of the derivative $Df(x_0)$ at the starting point. In 1955, Bartle showed, that in fact at every iteration x_k one can use the derivative $Df(z_k)$ instead of $Df(x_k)$, where z_k is any point in a neighborhood of x_0.
The Newton method has been extended in many directions: using approximations of $Df(z_k)$, versions for non-smooth functions, modifications for variational inequalities, etc.
In the paper to be presented we derive Kantorovich-type theorems for a generalized equation in Banach spaces X and Y: find a point $x \in X$ such that

$$f(x) + F(x) \ni 0,$$

where $f : X \to Y$ is a continuous function and $F : X \rightrightarrows Y$ is a set-valued mapping with closed graph. Many problems can be formulated in this way, for example, equations, variational inequalities, constraint systems, as well as optimality conditions in mathematical programming and optimal control. We present a Kantorovich-type theorem concerning linear, superlinear and quadratic convergence for a general algorithmic strategy covering both nonsmooth and smooth cases. At every step a "linearized" generalized equation of the form

$$f(x_k) + A_k(x - x_k) + F(x) \ni 0$$

has to be solved, where A_k is a bounded linear operator appropriately related to the function f. A condition for metric regularity of the mapping in the left hand side with $k = 0$ replaces the Kantorovich condition of invertibility of $Df(x_0)$.
Examples and computational experiments illustrate the theoretical results.

Decision Support Tool in the Project LANDSLIDE

Nina Dobrinkova

LANDSLIDES occur in many different geological and environmental settings across Europe and are a major hazard in most mountainous and hilly regions. Every year landslides cause fatalities and large damage to infrastructure and property. Intense and/or long lasting rainfall represents the most frequent trigger of landslides in Europe, and is expected to increase in the future due to climate change.

Methods for landslide evaluation are today mainly based on scientific literature of geomorphologic studies and of historical landslide events which do not consider or more often underestimate the impact of climate change.Therefore, it is important adaptation of computer based tools that can adapt to the new conditions by correctly evaluating and predicting landslide hazards which is a fundamental prerequisite for accurate risk mapping and assessment and for the consequent implementation of appropriate prevention measures.

LANDSLIDE is a European project, financed by the Directorate General Humanitarian Aid and Civil Protection of the European Commission, with the aim to develop an innovative risk assessment tool to predict and evaluate landslide hazards. Its focus is on calculations of risk maps for the responsible authorities in different test cases in Bulgaria, Italy, Greece and Poland. The simulations are applicable for landslides with twenty meters depth and the triggering cause for their activation is heavy rain falls.

The LANDSLIDE activities planned in the framework of the project are divided in three different action phases:

The first action phase, concerns the development of the Landslide Hazard Assessment Model and Software. All project partners have selected the four hydrographic basins (test sites) and started collecting both geomorphological and meteorological data needed to create a common database for correct adaptation and fine-tuning of the model to the selected test areas.

In the second phase the civil protection partners need to test and use the model and the software within their daily work by risk mapping and assessment activities. This will be preceded by a training course for the civil protection staff of the partner territories involved. During the pilot phase a help desk will also be established to support partners in correctly using and applying the model and software.

The third phase concerns the creation of a sustainable approach to risk prevention in each pilot territory to involve other relevant services and sectors concerned (agriculture, urban, etc.) to share the new risk maps, inform about risk scenarios and to

make risk prevention part of development policies and plans cross-sectors.

The main expected results from the LANDSLIDE project are:

- improve the capacity to elaborate more correct medium and long-term risk forecasts and risk scenarios and to schedule more appropriate prevention and mitigation measures for potential elements at risk.

- support the transfer of experience to other local and regional authorities, thanks to instruments and tools already tested and produced to facilitate the use and application of the model outside the test areas.

- integrate risk prevention and risk management considerations into planning and development of policies cross sectors.

- improve the capacity of the risk groups identified to know how to access risk information and how to engage in self-protection and prevention activities.

- foster a culture of prevention, both cross-sectors and at different levels, i.e. also at private and individual level.

In our article we will describe the system architecture and used parameters in order to have our risk maps as accurate as possible taking into account all available weather and soil parameters.

Blood Flow Simulations Based on Medical Image Data

Wolfgang Fenz, Ivan Georgiev, Vania Georgieva

Cerebral aneurysms are dilations of arterial walls that can grow over time and, in case of rupture leads to dangerous hemorrhage. There are different reasons for aneurysm, such as hypertension, arteriosclerosis, and heredity. An efficient way to study the generation, development, and rupture of aneurysms is based on fluid-structure interaction type simulations.
We present a novel simulation system of the blood flow through intracranial aneurysms including its interaction with the surrounding vessel tissue [1]. It enables physicians to estimate rupture risks by calculating the distribution of blood pressure, velocity and wall stresses in the aneurysm, in order to support the planning of clinical interventions [2].

Figure 1: Blood vessels geometry (left), mesh generation at the region of interest (right).

For the numerical simulation, the computational domain is extracted from high resolution medical image data of the patient's cerebrovascular system. The blood is modeled as an incompressible Newtonian fluid, and the surrounding vessel wall as an isotropic linear elastic material. Both the Navier-Stokes equations for the fluid domain and the Navier-Lame equations for the solid domain are handled with a finite element method, and the resulting linear equation systems are solved via and algebraic multigrid algorithm. Implicit coupling between blood flow and wall elasticity is achieved using an iterative fluid-structure interaction technique deforming the fluid mesh according to the wall displacement in each step. Boundary conditions are applied by prescribing measured waveforms of blood velocity and pressure at inlet and outlet areas.

Due to the time-critical nature of the application, we exploit efficient state-of-the-art numerical methods and high performance computing on advanced heterogeneous CPU-GPU extremely parallel architectures [3].

Acknowledgment This work is partially supported by the Bulgarian National Science Fund, grant DFNI-I02/3.

References

[1] MEDVIS 3D, http://www.medvis3d.at/

[2] Xiang et al., Stroke 2011, 42:144-152

[3] Parallel Toolbox, http://paralleltoolbox.sourceforge.net/

Generalized Net Model of Transportation Network

Stefka Fidanova, Krassimir Atanasov

There is different methods for transportation from one location to another one (trains, buses, aircrafts). The model of public transport can help for its organization and optimization. The railway transport (excluding the high speed trains with velocity more than 200 km/h) is slower, but cheaper. The buses and fast trains are faster, but with high price. Modeling transportation network we need to take in to account both the speed and the price of every one of the vehicle in every segment of their path. It is important to know how many passengers will prefer the train and how many will prefer the bus when the timetable is fixed and how the passenger flow will change if the timetable will be changed. Such a model can show where is more appropriate to invest, to improve the transportation system.

The oldest public transport, which is used now days, is the railway. The bus transport is a concurrent of the rail transport, because it is more flexible and can be faster. There exist different kinds of transportation models. The importance and role of each type of models is discussed in relation of its function. Some of the models are concentrated on scheduling. Other models are focused on simulation to analyze the level of utilization of different types of transportation. There are models which goal is optimal transportation network design.

In this work we propose a model of the public transport with Generalized Nets. Generalized Nets (GN) are extension and generalization of Petri nets. They are powerful tool for universal description of models of complex systems with many different and in most of the cases not homogeneous components, with simultaneous activities. The static structure consists of objects called **transitions**, which have input and output **places**. Two transitions can share a place, but every place can be an input of at most one transition and can be an output of at most one transition.

The dynamic structure consists of **tokens**, which act as information carriers and can occupy a single place at every moment of the GN execution. The tokens pass through the transition from one input to another output place; such an ordered pair of places is called **transition arc**. The tokens' movement is governed by conditions (predicates), contained in the **predicate** matrix of the transition.

The information carried by a token is contained in its **characteristics**, which can be viewed as an associative array of characteristic names and values. The values of the token characteristics change in time according to specific rules, called **characteristic functions**. Every place possesses at most one characteristic function, which assigns new characteristics to the incoming tokens. Apart from movement in the net and change of the characteristics, tokens can also split and merge in the places. A transition can contain m input and n output places where $n, m \geq 1$.

The GN are expandable. Every place can be replaced with new GN. Thus the process described by GN can be developed and complicated on more deeper level. The GN can help us to understand the processes and to see possibilities for their optimization.

In our model every station will be represented by transition. Several tokens will entry

the transition with different characteristics as number of passengers, number and type of the vehicles and their capacity, time and price of the vehicle to go from one station to another one.

Parallel Genetic Algorithms on Intel MIC Architecture

Dobromir Georgiev, Todor Gurov, and Emanouil Atanassov

Genetic Algorithms (GA) are metaheuristic search methods, inspired by biological evolution and genetics. By executing a heuristic search, they are able to find good solutions in reasonable time [1]. With the increase in the fitness landscape complexity, size of the search space, and complexity of the genetic representation, however, their efficiency rapidly deteriorates. An effective approach to improve the performance of GAs when tackling complex problems is through the usage of parallel computing architectures [2].

The Intel Many Integrated Core (Intel MIC) architecture is a coprocessor architecture developed by Intel that quickly gained traction and made its way into the leading TOP500 supercomputers. It provides two main programming models: offload, where program hotspots are identified and offloaded to the device, and native, where the entire application runs on the device [4].

For GAs where the fitness function is responsible for the greater part of the execution runtime, the heterogeneous offload programming model is often more suitable, as it is simpler to implement and does not result in any changes in the algorithm behaviour. However, for GAs that do not meet this criterion, an alternative parallelization scheme is required to fully utilize the target hardware. Here, we focus on the more general case - running GAs in native mode.

In this work we present an implementation of a distributed genetic algorithm (DGA) [3], tuned for execution on the Intel Xeon Phi. In our DGA, we execute a number of separate GA instances, which evolve separately, and exchange genetic information through the process of migration. Migration is an evolutionary operator, which enables distinct GA instances to share individuals. The migration is implemented in terms of point-to-point asynchronous MPI communications.

One of the key features of the Intel MIC architecture is the SIMD engine provided in each core. With vectors of width 512 bits, utilizing it is vital for gaining maximal performance from the coprocessor. Although the Intel Compilers are fairly good at detecting loops that may be vectorized, more often than not, it is up to the programmer to help the compiler detect opportunities for vectorization, or even to force the compiler to vectorize some loops. *#pragma IVDEP* and *#pragma VECTOR* are two directives that attempt to hint to the compiler that the loops they are applied on may be vectorized. For a more direct approach, *#pragma SIMD* and *#pragma vector always* force the compiler to vectorize the loop. In order to be fully aware of what the compiler has and has not vectorized, the compiler flags *-qopt-report-qopt-report-phase = vec* provide detailed reports on vectorization.

The presented results were obtained using the HPCG cluster at the Institute of Information and Communication Technologies at the Bulgarian Academy of Sciences, namely its Intel Xeon Phi-equipped servers, each containing 2 Intel Xeon E5-2650V2 processors and 8 Intel Xeon Phi 5110P devices. Each Intel Xeon Phi device, provides

60 cores. The experiments are focused on stress-testing the efficiency of the implementation and use the 3-SAT benchmark problem. The population contains binary vectors and is of size 200, migration occurs every 10 iterations and transfer 10% of the population.

Table 1: Troughput in terms of iterations per core.

Type Device	Number Cores	Number Processes	Iterartion per second per physical core
CPU	1	1	310
CPU	16	16	263
CPU	16	2 x 16	278
MIC	60	60	134
MIC	60	2 x 60	111
MIC	240	240	132
MIC	240	2 x 240	107
MIC	480	480	134
MIC	480	2 x 480	115

Despite requiring some manual annotations and optimizations, the MIC implementation of a DGA demonstrated excellent results in terms of scalability. This is achieved even for GAs with fitness functions with almost negligible runtime, which result in a higher communication to computation ratio. Asynchronous migrations do not affect the overall effectiveness of the GA, and enable streamlined computations. The implemented techniques can be applied to other evolutionary algorithms, including such that require shared knowledge between each algorithm instance. Additionally, adaptive population sizes may be implemented in order to utilize the CPU and the MIC in a single run, while keeping them in sync in terms of number of iterations.

Acknowledgments: This work was supported by the National Science Fund of Bulgaria under Grant DFNI-I02/8.

References:

[1] D. E. Goldberg, "Genetic Algorithms in Search, Optimization and Machine Learning", Addison-Wesley Longman, London, 2006.
[2] Eroftiev, A. A., et al., "Parallel computing in application to global optimization problem solving", 34th MIPRO2011 Proceedings, pp. 185-190, 2011.
[3] D. Georgiev, et al., A framework for parallel genetic algorithms for distributed memory architectures, ScalA '14 Proceedings of the 5th Workshop on LASA for LSS, pp. 47-53, IEEE 2014.
[4] J. Jeffers, J. Reinders; "Intel Xeon Phi Coprocessor High Performance Programming", Published by ELsevier Inc, pp. 409, 2013, ISBN:978-0-12-410414-3.

Volume Constraint Segmentation of Porous Media

Ivan Georgiev, Stanislav Harizanov, Svetozar Margenov, Yavor Vutov, Ludmil Zikatanov

Experimental measurements of macro characteristics of porous materials could be rather expensive and not always possible. In such cases, virtual material design is a modern research direction that significantly speeds up the analysis and the derivation of new porous materials with a priori given physical properties. A key topic in the investigation of advanced methods, algorithms and innovations based on 3D digitalization and prototyping is the voxel data processing of the input image.

Accurate segmentation of 3D CT data of porous media is crucial for the numerical simulations and the computation of the material/object's macro characteristics at the next stage. Due to the highly irregular structure of the segmentation phases and the presence of noise in the image, classical methods are not reliable and the results between different standard algorithms may differ drastically (even on up to 50% of the data).

We investigate a completely new direction of image segmentation, where the physical properties of the scanned specimen are incorporated in the mathematical model as constraints. In particular, the volume of the solid phase can be determined from the material's density and weight measurements and can be a priori fixed, while the solid phase itself should be connected whenever the specimen is a single material piece.

Two different families of 2-phase image segmentation methods have been proposed, analyzed and implemented. The first is based on graph 2-Laplacian and guarantees exact volume reconstruction of the solid phase. The second approach preserves both the volume and the connectivity of the solid phase and is based on the minimum spanning tree (MST) properties of a weighted graph. The edge weights in both the graphs are induced by the input image data and measure similarities between neighboring voxels.

The conducted numerical experiments are promising in terms of both improved accuracy and decreased computational time. MPI parallel implementations of the new algorithms are developed in order to further optimize their efficiency.

On Generalized Fourier Transforms for Nonlocal Nonlinear Evolution Equation

Vladimir S. Gerdjikov

We start with the generic AKNS system

$$L\psi \equiv i\frac{d\psi}{dx} + (q(x,t) - \lambda\sigma_3)\,\psi(x,t,\lambda) = 0, \qquad q(x,t) = \begin{pmatrix} 0 & q_+ \\ q_- & 0 \end{pmatrix}. \tag{1}$$

whose potential $q(x,t)$ belongs to the class of smooth functions vanishing fast enough for $x \to \pm\infty$. By generic here we mean that the complex-valued functions $q_+(x,t)$ and $q_-(x,t)$ are independent. Using L as a Lax operator we can integrate a system of two equations for $q_+(x,t)$ and $q_-(x,t)$ generalizing the famous NLS eq. (GNLS). After the reduction $q_+(x,t) = q_-^*(x,t)$, this system reduces to the NLS eq.; applying different 'nonlocal' reduction $q_+(x,t) = \epsilon q_-^*(-x,t) = u(x,t)$, $\epsilon^2 = 1$ we obtain the nonlocal NLS [1]:

$$i\frac{\partial u}{\partial t} + \frac{1}{2}\frac{\partial^2 u}{\partial x^2} + \epsilon u^2(x,t)u^*(-x,t) = 0. \tag{2}$$

which also finds physical applications.

We prove that the 'squared solutions' of L (1) form complete set of functions thus generalizing the results of [5, 3], see also [4]. Then, using the expansions of $q(x,t)$ and $\sigma_3 q_t(x,t)$ over the 'squared solutions we extend the interpretation of the ISM as a generalized Fourier also to the NLEE related to L with nonlocal reduction. Next we introduce a symplectic basis [2], which also satisfies the completeness relation and denote by $\delta\eta(\lambda)$ and $\delta\kappa(\lambda,t)$ the expansion coefficients of $\sigma_3\delta q_t$ over it. If we consider the special class of variations $\sigma_3\delta q(x) \simeq \sigma_3 q_t \delta t$ then the expansion coefficients $\delta\eta(\lambda) \simeq \eta_t\delta t$ and $\delta\kappa(\lambda,t) \simeq \kappa_t\delta t$. If $q(x,t)$ is a solution to the GNLS system we get:

$$\frac{\partial\eta(\lambda)}{\partial t} = 0, \qquad \frac{\partial\kappa(\lambda,t)}{\partial t} = 2\lambda^2,$$

i.e. the variables $\eta(\lambda)$ and $\kappa(\lambda,t)$ may ne understood as the action-angle variables for the generalized NLS system.

Finally, if we apply the local involution $q_+(x,t) = q_-^*(x,t) = u(x,t)$ we recover the well known action-angle variables of the NLS eq. If we apply the nonlocal involution $q_+(x,t) = q_-^*(-x,t) = u(x,t)$ we obtain the action-angle variables of the nonlocal NLS (2) in terms of the scattering data of L.

These results can be generalized also to Zakharov-Shabat type operators

$$\begin{aligned} L\psi &\equiv i\frac{d\psi}{dx} + (Q(x,t) - \lambda J)\,\psi(x,t,\lambda) = 0, \\ Q(x,t) &= \sum_{\alpha\in\Delta_+} (q_\alpha(x,t)E_\alpha + p_\alpha(x,t)E_{-\alpha}), \qquad J = \sum_j a_j H_j, \end{aligned} \tag{3}$$

where Δ_+ is the set of positive roots of the simple Lie algebra $\mathfrak{g}$ and E_α and H_j are the Cartan-Weyl generators of $\mathfrak{g}$.
Next it will be demonstrated that 'squared solutions' of L (3) satisfy the completeness relations also in the cases when $U(x,t,\lambda) = Q(x,t) - \lambda J$ satisfy each of the two types of non-local reductions

$$\begin{aligned} &\text{A)} \qquad C_1^{-1} U^\dagger(x,t,\kappa_1\lambda^*) C_1 = U(-x,-t,\lambda), \\ &\text{B)} \qquad C_2^{-1} U^\dagger(x,t,\kappa_2\lambda^*) C_2 = U(-x,t,\lambda), \end{aligned} \tag{4}$$

where C_1 and C_2 are two involutive automorphisms of $\mathfrak{g}$ and $\kappa_k = \pm 1$, $k = 1, 2$.

References

[1] M. Ablowitz and Z. Musslimani, Integrable Nonlocal Nonlinear Schrödinger Equation, Phys. Rev. Lett., 110 (2013) 064105(5).

[2] V. S. Gerdjikov, A. Saxena. Complete integrability of Nonlocal Nonlinear Schrödinger equation. **arXiv:1510.00480v1 [nlin.SI]**.

[3] V. S. Gerdjikov, E. Kh. Khristov. *On the evolution equations solvable with the inverse scattering problem. II. Hamiltonian structures and Backlund transformations.* Bulgarian J. Phys. **7,** No.2, 119–133, (1980) (In Russian).

[4] V. S. Gerdjikov, G. Vilasi, A. B. Yanovski. *Integrable Hamiltonian Hierarchies. Spectral and Geometric Methods* Lecture Notes in Physics **748**, Springer Verlag, Berlin, Heidelberg, New York (2008). ISBN: 978-3-540-77054-1.

[5] D.J. Kaup, *Closure of the Squared Zakharov-Shabat Eigenstates*, J. Math. Analysis and Applications **54**, No. 3, 849-864 (1976).

Supervised 3D-Surface Fitting

Stanislav Harizanov, Ivan Georgiev, Svetozar Margenov

Computer-aided design (CAD) is used in many fields such as electronic systems, mechanics, technical drawing, etc. Referring to [1] *"CAD software is used to increase the productivity of the designer, improve the quality of design, improve communications through documentation, and to create a database for manufacturing"*. Nowadays, it has numerous applications, including in automotive, shipbuilding, and aerospace industries, industrial and architectural design, prosthetics, and computer animation. Because of its enormous economic importance, CAD has been a major driving force for research in computational geometry, computer graphics (both hardware and software), and discrete differential geometry [2].
The goal of this paper is to *efficiently* extract *correct* 3D-surface information for *particular* CAD-modeled details from both their laser scan and industrial CT scan reconstructions. Unlike general and standard data fitting algorithms, our procedure incorporates specific additional feature information for the input object, thus the quality of the output mesh is improved, its complexity is significantly reduced, and its surface geometry approximates well the original detail geometry. Noise is removed as well as other artifacts that appear during the scanning process.

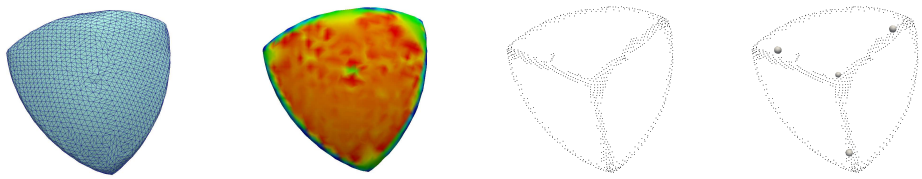

Figure 1: From left to right: The detail 3D original triangulated mesh after laser scanning. The discrete Gaussian curvature diagram at the mesh knots. High curvature mesh knots. The corresponding centers of the K-means algorithm w.r.t. them for $k = 4$.

As an illustration, consider the detail from Fig 1. The manufacturer has told us this should be a "spherical tetrahedron", i.e., 4 spherical triangles, glued together. We are given a fine-scale triangulated mesh, obtained from the point-cloud data derived by the laser scanning of a particular specimen and we want

1. To add the pattern shape to the CAD database.
2. To check the quality of the specimen (if it is defected or not).

The input file is in `.stl` format, where we have a list of all the planar triangular patches, represented via the 3D coordinates of their vertices. We can shift to NURBS geometry (the building block of the CAD system) directly on the input mesh and

derive a CAD model for the detail, but this will lead to 4562 knots and 9098 different faces, which is not only extremely inefficient storage-wise but also not the exact shape pattern as the potential specimen's defects and the inevitable reconstruction artifacts have been taken into account.
Instead, we'd better locate the 4 vertices of the specimen, generate a very simple mesh, consisting of only 4 triangles, and take "the best sphere fit" (for example in a least squares sense) for each patch. Note that spheres are within the NURBS class, thus CAD-compatibility is achieved. Therefore, our modeling task simplifies to closely approximating the 4 vertices and the 6 (arc) edges of the tetrahedron. A possible solution is illustrated on Fig. 1, where standard public software was used. For each vertex of the original mesh we compute its discrete Gaussian curvature, using the filter *Colorize Curvature APSS* in MESHLAB [3]. The vertex color relates to the curvature magnitude. The mesh knots on the tetrahedron edges are expected to be blue, while all the rest - to be red. Then, applying Principle Component Analysis (PCA) to the "blue point cloud" should give us exactly the 4 tetrahedron vertices, as the centers of the 4 different data components. In practice, however, this is not the case. Not only the thickness of the different edges differs, but there are also outliers within the 4 spherical patches. Thus, if we directly apply the k-means filter [4, 5] to the blue point cloud, the centers of the 4 components approximate poorly the tetrahedron vertices. In this work, we propose more advanced techniques for better vertex localization.

Acknowledgements

This research is partially supported by the project AComIn "Advanced Computing for Innovation", grant 316087, funded by the FP7 Capacity Program.

References

[1] Narayan, K.: Computer Aided Design and Manufacturing. New Delhi: Prentice Hall of India (2008)

[2] Pottmann, H., Brell-Cokcan, S., Wallner, J.: Discrete surfaces for architectural design. In Curve and Surface Design, P. Chenin, T. Lyche, and L. Schumaker (eds.), 213–234, Nashboro Press (2007)

[3] MESHLAB. `http://meshlab.sourceforge.net` (2014)

[4] MacQueen, J.: Some Methods for Classification and Analysis of Multivariate Observations. Proc. Fifth Berkeley Symp. Math. Statistics and Probability 1, 281–296 (1967)

[5] Bezdek, J., Ehrlich, R., Full, W.: FCM: The fuzzy c-means clustering algorithm. Computers & Geosciences 10(2-3), 191–203 (1984)

Optimal Multigrid Methods for H(div)-Conforming Discontinuous Galerkin Discretizations of the Brinkman Problem

Qingguo Hong, Johannes Kraus

We consider discontinuous Galerkin $H(div,\Omega)$-conforming discretizations of elasticity type and Brinkman equations. We analyze their uniform stability and describe a simple Uzawa iteration for the solution of the Brinkman problem

$$\begin{cases} a_h(\boldsymbol{u}_h,\boldsymbol{v}_h)+b_h(\boldsymbol{v}_h,p_h)=(\boldsymbol{f},\boldsymbol{v}_h), \quad \text{for all} \quad \boldsymbol{v}_h\in\boldsymbol{V}_h,\\ b_h(\boldsymbol{u}_h,q_h)=(g,q_h), \quad \text{for all} \quad q_h\in S_h, \end{cases} \tag{1}$$

where

$$\begin{aligned} a_h(\boldsymbol{u},\boldsymbol{v}) &:= \epsilon^2\Big(\sum_{K\in T_h}\int_K \varepsilon(\boldsymbol{u}):\varepsilon(\boldsymbol{v})dx-\sum_{e\in E_h}\int_e\{\varepsilon(\boldsymbol{u})\}\cdot[\boldsymbol{v}_t]ds\\ &\quad -\sum_{e\in E_h}\int_e\{\varepsilon(\boldsymbol{v})\}\cdot[\boldsymbol{u}_t]ds+\sum_{e\in E_h}\int_e\eta h_e^{-1}[\boldsymbol{u}_t]\cdot[\boldsymbol{v}_t]ds\Big)+\rho^2\int_\Omega \boldsymbol{u}\boldsymbol{v}\,dx,\\ b_h(\boldsymbol{u},q) &:= \int_\Omega \nabla\cdot\boldsymbol{u}q\,dx, \end{aligned}$$

and η is a properly chosen penalty parameter independent of the mesh size h such that $a_h(\cdot,\cdot)$ is positive definite.
The Uzawa method with damping parameter $\lambda\gtrsim 1$ for solving problem (1) reads: Given $(\boldsymbol{u}_h^l,p^l)$, compute $(\boldsymbol{u}_h^{l+1},p^{l+1})$ as the solution of the system

$$\begin{aligned} &a_h(\boldsymbol{u}_h^{l+1},\boldsymbol{v}_h)+\lambda(\operatorname{div}\boldsymbol{u}_h^{l+1},\operatorname{div}\boldsymbol{v}_h)=(\boldsymbol{f},\boldsymbol{v}_h)-b_h(\boldsymbol{v}_h,p_h^l)+\lambda(g,\operatorname{div}\boldsymbol{v}_h),\\ &p_h^{l+1}=p_h^l-\lambda\operatorname{div}\boldsymbol{u}_h^{l+1}-\lambda g, \end{aligned}$$

for all $\boldsymbol{v}_h\in\boldsymbol{V}_h$. Obviously, the major part of the computational work for executing this algorithm is spent on solving in every iteration a nearly incompressible linear elasticity type problem of the form: Find $\boldsymbol{u}_h\in\boldsymbol{V}_h$ such that

$$A_h(\boldsymbol{u}_h,\boldsymbol{v}_h)=(\boldsymbol{F},\boldsymbol{v}_h), \quad \text{for all} \quad \boldsymbol{v}_h\in\boldsymbol{V}_h, \tag{2}$$

where $A_h(\cdot,\cdot)$ is defined by

$$A_h(\boldsymbol{u}_h,\boldsymbol{v}_h):=a_h(\boldsymbol{u}_h,\boldsymbol{v}_h)+\lambda(\operatorname{div}\boldsymbol{u}_h,\operatorname{div}\boldsymbol{v}_h).$$

Based on a special subspace decomposition of $H(div,\Omega)$, we analyze variable V-cycle and W-cycle multigrid methods with non-nested bilinear forms for solving problem (2). We prove that these algorithms are robust and their convergence rates are independent of the material parameters such as Lamé parameters and Poisson ratio and of the mesh size. Numerical results that confirm the theoretical analysis are presented. This is a joint work with Qingguo Hong (RICAM, Austrian Academy of Sciences).

Standing Waves in Systems of Perturbed Sine-Gordon Equations

Radoslava Hristova, Ivan Hristov

We consider the following system of perturbed Sine-Gordon equations:

$$S(\varphi_{tt} + \alpha\varphi_t + \sin\varphi - \gamma) = \varphi_{xx}, \quad 0 < x < L.$$

Here S is the $N \times N$ cyclic tridiagonal matrix

$$S = \begin{pmatrix} 1 & s & 0 & . & 0 & s \\ s & 1 & s & 0 & . & 0 \\ . & . & . & . & . & . \\ . & . & . & . & . & . \\ 0 & . & 0 & s & 1 & s \\ s & . & 0 & 0 & s & 1 \end{pmatrix}$$

The unknown is the column vector $\varphi = (\varphi_1, ..., \varphi_N)^T$. The system is solved numerically by a leapfrog difference scheme together with appropriate initial conditions and with Neumann boundary conditions:

$$\varphi_x(x = 0, L) = 0.$$

The parameters are α, γ, L, s. Depending on the values of the parameters we show the existence of standing wave solutions with synchronized (in-phase) waves for each equation. We show that the recent experiments on powerful THz radiations from mesas of BSCCO single crystals can be explained in terms of these solutions.
We also solve numerically the 2D generalization of the above system and analyze the achieved 2D standing waves. The system is considered on rectangular domains with different aspect ratio. For the investigation with respect to the parameters and solving the 2D problem we use the computational resources of IICT-BAS. The constructed numerical algorithms serve as a good examples for testing the different platforms of the heterogeneous cluster of IICT-BAS. The results of these tests are analyzed.

Stability Analysis of an Inflated Thin-Walled Hyperelastic Tube with Application to Abdominal Aortic Aneurysms

Tihomir Ivanov, Elena Nikolova

The abdominal aortic aneurysm is a local dilatation of the lower part of the aorta due to the weakening of the vessel wall. In many cases its rupture causes massive bleeding with associated high mortality. Recently, one of the main hypotheses for initiation and progress of aneurysms is connected with appearance of mathematical instabilities in the quasi-static response of the aneurysmal wall, depending on its specific material properties, i.e. the corresponding constitutive equation.

In this study we consider the inflation of the arterial/aneurysmal wall subjected to a constant blood pressure. The arterial/aneurysmal wall is modeled as a thin-walled, incompressible, hyperelastic and isotropic cylindrical membrane, as its motion can be presented by the following second-order ordinary differential equation:

$$\frac{\rho H R}{\lambda^2}\frac{d\lambda^2}{d^2t} = P(t) - \frac{T(\lambda)}{\lambda R} \tag{1}$$

where λ is the stretch ratio of the wall, ρ is its mass density, H is the underformed thickness of the wall, R is the underformed arterial/aneurysmal radius, $P(t)$ is the arterial blood pressure, which is assumed to be a constant, and $T(\lambda) = HS$ is the principal stress resultant. The hyperelasticity of the arterial/aneurysmal wall can be presented in the following manner:

$$S_i = \frac{dW}{dE_i}, \quad (i = 1, 2) \tag{2}$$

where $S_{1,2}$ are the Piola–Kirchhoff stresses, $E_{1,2}$ are the Green strains, and W is the strain energy function (SEF), respectively. For an isotropic material $S_1 = S_2$ and $E_1 = E_2$.

We examine the stability of the equilibria of Eq. (1), using four different forms of SEF, which principally describe the mechanical properties of rubber-like materials, but they are applied in modeling the hyperelastic response of biological soft tissues (including the arterial/aneurysmal wall) to external loads, as well. It is proved that the elastic stability or instability of the wall material is associated with mathematical monotonicity or non-monotonicity of the pressure-stretch relation. We define two types of instabilities in dependence on the material parameters and the analytical form of SEF. The first type is connected with the notion of 'limit point instability' associated with existence of a global maximum of the equilibrium pressure, at which a diametrical inflation of the arterial/aneurysmal wall only is realized. This case can

be explained by the well-known 'party balloon effect', at which the stretch continues to increase in presence of a decreasing pressure. The second type of instability is connected with the notion of 'an inflation jump', which is characterized by presence of a local maximum, followed by a local minimum, which can be followed again by an increasing pressure-stretch curve. In this case, once the maximum is reached, and the pressure is increased, the stretch will 'jump' to a significantly higher value, and an 'inflation propagation' is observed, that is there is an axial expansion of the arterial tube, as well.

In this study we prove analytically that the stable inflation of the arterial/aneurysmal tube can retain or can change to unstable one depending on the concrete analytical form of SEF and its material parameters. Moreover, we determine the boundary values of the parameters, where the limit point instability or the inflation jump can appear or disappear.

Acknowledgements: This research was supported by the project FNI I– 02/3.

On the Dynamics of Internal Waves in the Presence of Currents

Rossen Ivanov, Alan Compelli

We examine a two-media 2-dimensional fluid system consisting of a lower medium bounded underneath by a flatbed and an upper medium with a free surface with wind generated surface waves but considered bounded above by a lid by an assumption that surface waves have negligible amplitude. An internal wave driven by gravity acts as a free common interface between the media. The current is such that it is zero at the flatbed and with a profile consistent with the assumption that surface winds blow in the negative x-direction (at the lid). We are concerned with the layers adjacent to the internal wave in which there exists a depth dependent current, see Fig. 1 and [3]. Both media are considered incompressible and having either zero or non-zero constant vorticities. We consider a velocity field in layers II and III as (cf. [4, 1, 2])

$$\begin{cases} u_i = \tilde{\varphi}_{i,x} + \gamma y + \kappa \\ v_i = \tilde{\varphi}_{i,y}. \end{cases} \tag{1}$$

where $\tilde{\varphi}_i$ is the fluid potential in Ω_i due to wave motion, γ is the constant vorticity, due to the linear current profile in the layers and κ is a constant, representing the current velocity at $y = 0$. ρ_1 and ρ_2 are the respective constant densities of the lower and upper media and stability is given by the immiscibility condition $\rho_1 > \rho_2$. We assume that for large $|x|$ the amplitude of η attenuates and hence make the following assumptions $\lim_{|x|\to\infty} \eta(x,t) = 0$, $\lim_{|x|\to\infty} \tilde{\varphi}_i(x,y,t) = 0$, and $-l_1 < \eta(x,t) < l_2$ for all x and t i.e. the wave is localised in the *strip*. The Euler's equation leads to the Bernoulli condition (cf. [1, 2]), giving the time evolution of $\tilde{\varphi}_i$ at the interface. The kinematic condition for the interface gives the time evolution of $\eta(x,t)$.
The governing equations could be written in canonical Hamiltonian form in terms of the variables, associated to the wave (in a presence of a constant current). The resultant equations of motion show that wave-current interaction is influenced only by the current profile in the strip adjacent to the internal wave. The case $\gamma = 0$ is studied in [5].

References

[1] A. Compelli. Hamiltonian formulation of 2 bounded immiscible media with constant non-zero vorticities and a common interface. *Wave Motion* **54** (2015), 115–124.

[2] A. Compelli. Hamiltonian Approach to the Modeling of Internal Geophysical Waves with Vorticity. *Monatshefte für Mathematik* **TBD** (2015), http://arrow.dit.ie/scschmatart/178/.

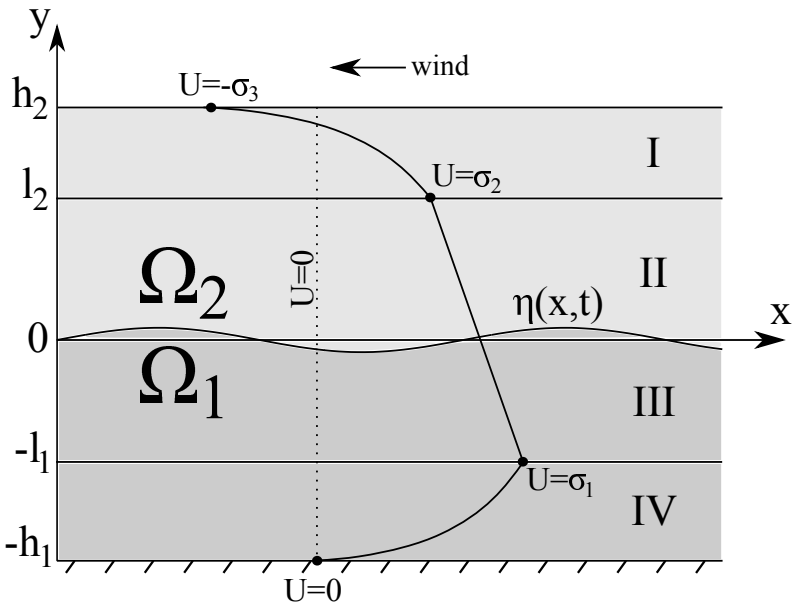

Figure 1: System setup. The current profile in layers I and IV is arbitrary as we are only concerned with layers II and III as the internal wave is a free interface between these layers. $U(y)$ is linear in layers II and III and continuous in layers I and IV.

[3] A. Constantin, R. Johnson. The dynamics of waves interacting with the Equatorial Undercurrent. *Geophysical & Astrophysical Fluid Dynamics* **109** (2015), 311-358.

[4] A. Constantin, R. Ivanov. A Hamiltonian Approach to Wave-Current Interactions in Two-Layer Fluids. *Physics of Fluids* **27**, *4* (2015), DOI: 10.1063/1.4929457.

[5] A. Compelli, R. Ivanov. On the dynamics of internal waves interacting with the equatorial undercurrent. *J. Nonlin. Math. Phys.* **22** (2015), 531–539; arXiv:1510.04096 [math-ph]

Efficient Option Valuation of Single and Double Barrier Options

Stanimir Kabaivanov, Mariyan Milev, Angel Marchev Jr.

In this paper we present an implementation of pricing algorithm for single and double barrier options and its suitability for real-world applications. A detailed analysis of the applied algorithm is accompanied by implementation in C++ (source code included) that is then compared to existing solutions in terms of efficiency and computational power. We then compare the applied method with existing closed-form solutions and well known methods of pricing barrier options that are based on finite differences.
Accurate and efficient barrier option valuation is important for solving a wide range of financial problems that spread beyond the scope of derivative markets. Real options analysis and investment opportunities study are just a few of the areas that can also benefit from the development of open and transparent procedures for valuation that are designed with three important features in mind – open access to the calculation algorithms, flexibility and usability.
In this paper we present an implementation of a pricing algorithm for single and double barrier options and focus on its sustainability for real world applications. Although there are many similar implementation available the one shown here is different in the following ways – it uses Mellin transform for option pricing as discussed in [1] and an algorithm developed in [2]; the main focus is put on providing sufficient accuracy while maintaining very small error rates and keeping the calculation time low; code is completely open and relies only on open packages which means that it can be used freely and without limitations or licensing issues.
The implementation is then tested for accuracy and efficiency against the following widely used valuation methods:

- Modified Black-Scholes equation which needs to be solved with additional limitations regarding possible changes in the underlying asset price S:

$$\frac{\partial C}{\partial t} + \frac{1}{2}\sigma^2 S^2 \frac{\partial^2 C}{\partial S^2} + rS\frac{\partial C}{\partial S} - rS = 0,$$

where contrary to the vanilla option case, important S values are bound by the upper and lower barriers (depending also on the option type). Within this context, the major factor during the comparison is the accuracy improvement brought by the implementation discussed in our paper.

- Finite difference method that can be used to reduce the modified equation solution to solving a linear equations system, as this makes it easier to solve more complex cases at the expense of increased calculation time.

Within this context we try to demonstrate that implementation based on algorithm suggested in [2] can be faster, while keeping sufficient accuracy and can outperform FDM approach.

- Lattice methods based on binomial trees where solution is also approximated with simple discretization and split up of the observed interval into finite small periods.

Although binomial trees can be applied for barrier options with complex structure (and in particular changes in the barrier level) they are prone to very slow convergence of the results, as discussed in detailed in [3].

- Monte Carlo methods that are able to support valuation of very complex options but at the expense of lengthy calculations.

Depending on the number of simulated scenarios, Monte Carlo methods may not be suitable for practical use, regardless of the fact that we can obtain very accurate results.
When comparing the implemented method we have used C++ with boost libraries [4], Eigen for linear algebra [5] and QuanLib [6] for comparison with popular open source implementations of finite difference methods and Black-Scholes analytical solutions.

References

[1] L. Jodar, P. Sevilla-Peris, J. C. Cortes and R. Sala, "A new direct method for solving the Black–Scholes equation," Appl. Math. Lett., vol. 18, no. 1, pp. 29-32, 2005.

[2] H. Gzyl, M. Milev and A. Tagliani, "Discontinuous payoff option pricing by Mellin Transform: A probabilistic approach," 2012.

[3] E. Derman, I. Kani, D. Ergener and I. Bardhan, "Enhanced Numerical Methods for Options with Barriers," Financial Analysts Journal, vol. 52, no. 4, pp. 25-36, 1996.

[4] "BOOST.ORG," 2015. [Online]. Available: http://www.boost.org/.

[5] "Eigen," 2015. [Online]. Available: http://eigen.tuxfamily.org/index.php?title=Main_Page.

[6] "QuantLib," [Online]. Available: http://quantlib.org/index.shtml.

Scalable High-Order Finite Elements for Compressible Hydrodynamics

Tzanio Kolev

The discretization of the Euler equations of gas dynamics ("compressible hydrodynamics") in a moving material frame is at the heart of many multi-physics simulation algorithms. The Arbitrary Lagrangian-Eulerian (ALE) framework is frequently applied in these settings in the form of a Lagrange phase, where the hydrodynamics equations are solved on a moving mesh, followed by a three-part "advection phase" involving mesh optimization, field remap and multi-material zone treatment.
This talk presents a general Lagrangian framework [1] for discretization of compressible shock hydrodynamics using high-order finite elements. The novelty of our approach is in the use of high-order polynomial spaces to define both the mapping and the reference basis functions. This leads to improved robustness and symmetry preservation properties, better representation of the mesh curvature that naturally develops with the material motion, significant reduction in mesh imprinting, and high-order convergence for smooth problems. We also discuss ongoing work on the application of the curvilinear technology to the "advection phase" of ALE, including a DG-advection approach for conservative and monotonic high-order finite element interpolation (remap), high-order extensions of classical mesh optimization algorithms, such as harmonic and equipotential smoothing and the use of high-order material indicator function for handling mixed elements in multi-material ALE problems.
In addition to their mathematical benefits, high-order finite element discretizations are a natural fit for future HPC hardware, because their order can be used to tune the performance, by increasing the FLOPs/bytes ratio, or to adjust the algorithm for different hardware. In this directtion, we present some of our work on scalable high-order finite element software that combines the modular finite element library MFEM [2], the hypre library of linear solvers [3], and the high-order shock hydrodynamics code BLAST [4]. We explain how the MPI-based version of MFEM uses data structures and kernels from the hypre library to enable scalable finite element assembly in parallel and describe the efficient implementation of high-order force matrices in the MFEM-based BLAST application, where we will also demonstrate the benefits of our approach with respect to strong scaling and GPU acceleration. Finally, we consider general non-conforming high-order adaptive refinement in MFEM with applications to compressible hydrodynamics in BLAST and computational electromagnetic problems.

References

[1] V. Dobrev and Tz. Kolev and R. Rieben, High-Order Curvilinear Finite Element Methods for Lagrangian Hydrodynamics, SIAM Journal on Scientific Computing, (34) 2012, pp.B606-B641.

[2] MFEM: Modular finite element library, http://mfem.org.

[3] hypre: Scalable linear solvers library, http://llnl.gov/casc/hypre.

[4] BLAST: High-order shock hydrodynamics, http://llnl.gov/casc/blast.

New Bounds for BER of Integer Coded TQAM in AWGN Channel

Hristo Kostadinov, Liliya Kraleva, Nikolai Manev

Abstract

We investigate the performance of coded modulation scheme based on the application of integer codes to triangular quadrature amplitude modulation (TQAM). An upper and a low bound for bit error probability (BER) in the case of AWGN channel are derived. These bounds are so closed that it makes the calculation of the exact value of BER unnecessary in practice.

1 Introduction

The term coded modulation means a combination of a scheme of coding and modulation techniques. Nowadays, in modern digital communication systems, high-order modulation is preferred for high-speed data transmission. One of the most popular modulation in commercial communication systems is square quadrature amplitude modulation (SQAM). SQAM scheme is easy to be implemented and has a good performance with simple detection.
Recently, the triangular quadrature amplitude modulation (TQAM) was proposed. A comparison of the two constellation, SQAM and TQAM, shows that TQAM is more power efficient than SQAM and preserves low detection complexity. In [3] was derived the general formula calculating the average energy per symbol of the TQAM. Also, in the same work was analysed the bit error rate (BER) of the TQAM over AWGN channel, without using any coding techniques.
Integer codes are codes defined over finite rings of integers. Their advantage over the traditional block codes, is that we can correct errors of a given type, which means that for a given channel and modulator we can choose the type of the errors (which are the most common) and after that construct integer code capable of correcting those errors. The application of integer codes in different modulation schemes, especially in QAM, are discussed in [1, 2].
Before finding tight bounds of BER for TQAM, we have investigated BER of SQAM. The reason is, that for SQAM we have the exact expression of BER. In Figure 1 is presented the comparison of BER of 16-SQAM between the exact formula of BER (SQAM-square), our lower and upper bounds (SQAM-cir2 and SQAM-cir1) and the average of the two bounds (SQAM-aver). From that results, we can conclude that SQAM-aver is very close (almost same) as the BER obtained by calculating of the exact formula. Also, Figure 1 shows same comparison for TQAM, only without the curve for the exact expression.
A comparison uncoded and coded by integer code 16-TQAM is shown in Figure 2. We notice that the lower, upper and average of the both bounds are same and can not be distinguished on the graphic. The coding gain in this case is more that 3 db.

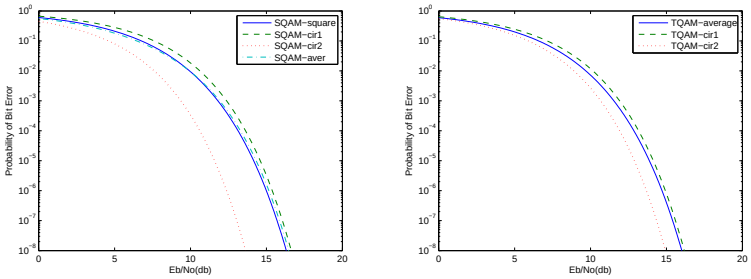

Figure 1: Probability of Bit Error (BER) for uncoded 16-SQAM and 16-TQAM

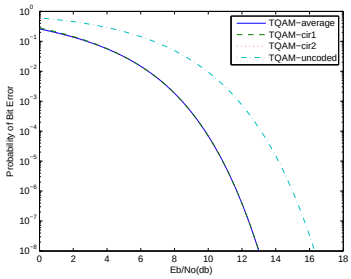

Figure 2: Probability of Bit Error for coded 16-TQAM

References

[1] H. Kostadinov, H. Morita and N. Manev: Derivation on Bit Error Probability of Coded QAM using Integer Codes. IEICE Trans. on Fundamentals, Vol. E87-A (12), 3397–3403 (2004)

[2] H. Kostadinov, H. Morita, N. Iijima, A.J. Han Vinck and N. Manev: Soft Decoding of Integer Codes and Their Application to Coded Modulation. IEICE Trans. on Fundamentals, Vol. E39-A (7), 1363–1370 (2010)

[3] Park, Sung-Joon: Performance Analysis of Triangular Quadrature Amplitude Modulation in AWGN Channel. IEEE Commun. Letters, Vol. 16, 765–768 (2012)

Geothermal Effects for BOD Removal in Horizontal Subsurface Flow Constructed Wetlands: A Numerical Approach

Konstantinos Liolios, Vassilios Tsihrintzis, Krassimir Georgiev, Ivan Georgiev

1 Introduction

Geothermal energy (heat) and mass transport through porous media are governing concepts concerning the operational modelling of geothermal reservoirs [1, 2, 3]. Such geothermal energy storage tools can be considered as the unconfined aquifers of Constructed Wetlands (CW) [4].
The traditional numerical simulation of CW operation is based on the concepts of groundwater flow and the contaminant transport and removal through porous media, under the assumption of isothermal conditions. Thus, an averaged constant temperature level is assumed during the time of operation required by the hydraulic residence time (HRT). But in reality, temperature is a variable quantity during HRT and is necessary to take into account its dependence on the decay coefficients.
A numerical simulation of Biochemical Oxygen Demand (BOD) removal in Horizontal Subsurface Flow (HSF) CW is presented under temperature variability. The computer code MODFLOW [5, 6, 7] is used, where finite-difference techniques are applied for the spatial and temporal discretization of the equations.

2 The mathematical formulation of the problem

The partial differential equation which describes the fate and transport of a contaminant with adsorption in 3D, transient groundwater flow systems, is:

$$\varepsilon R_d \frac{\partial C}{\partial t} = \frac{\partial}{\partial x_i}\left(\varepsilon D_{S_{ij}} \frac{\partial C}{\partial x_i}\right) - \frac{\partial}{\partial x_i}(q_i C) + q_s C_s + \sum R_n, \tag{1}$$

where ε is the porosity of the subsurface medium; R_d is the retardation factor; $D_{S_{ij}}$ is the solute hydrodynamic dispersion coefficient tensor, in $[\mathrm{L^2T^{-1}}]$; C_s is the concentration of the source or sink flux, in $[\mathrm{ML^{-3}}]$; q_s is the volumetric flow rate of aquifer, representing fluid sources (positive) and sinks (negative), in $[\mathrm{LT^{-1}}]$; and $\sum R_n$ is the chemical reaction term, in $[\mathrm{ML^{-3}T^{-1}}]$, which for the usual linear reaction case is given by the formula:

$$\sum R_n = -\lambda R_d C, \tag{2}$$

where λ is the first-order removal coefficient, in $[\mathrm{T^{-1}}]$. For usual solute removal in HSF CW, is considered that λ depends mainly on the temperature. Indeed, based on

experimental results, temperature effects have often been summarized by Arrhenius [8].
The above partial differential equations (1)-(2) describe the 3-dimensional flow of groundwater, the heat transport and the transport and removal of contaminants in a heterogeneous and anisotropic medium. The unknowns of the problem are: The hydraulic head: $h = h(x_i; t)$, the three velocity components: $q_i = q_i(x_i; t)$, the temperature: $T = T(x_i; t)$ and the concentration: $C = C(x_i; t)$.

3 The numerical treatment of the problem

The Finite Difference Method (FDM) is chosen for the numerical solution of the problem, which was described in the previous paragraph. FDM is the basis for the computer code MODFLOW [7], which is widely used for the simulation of groundwater flow and mass transport. Heat is considered as tracer according to [9].

References

[1] Bear, J.: Dynamics of Fluids in Porous Media. Dover Publications, New York (1988)

[2] De Marsily, G.: Quantitative Hydrogeology. Academic Press, London (1986)

[3] Lee, K. S.: A Review on Concepts, Applications and Models of Aquifer Thermal Energy Storage Systems. Energies 3, 1320-1334 (2010)

[4] Kadlec, R. H., Wallace, S.: Treatment Wetlands. 2nd Edition, CRC Press, Boca Raton, USA (2009)

[5] Liolios, K. A., Moutsopoulos, K. N., Tsihrintzis, V. A.: Modeling of Flow and BOD Fate in Horizontal Subsurface Flow Constructed Wetlands. Chemical Engineering J. 200-202, 681-693 (2012)

[6] Liolios, K., Tsihrintzis, V., Moutsopoulos, K., Georgiev, I., Georgiev, K.: A Computational Approach for Remediation Procedures in Horizontal Subsurface Flow Constructed Wetlands. In: Lirkov, I., Margenov, S., Wasniewski, J., (Eds.) LNCS, vol. 7116, pp. 299-306, Springer, Heidelberg (2012)

[7] Waterloo Hydrogeologic Inc.: Visual MODFLOW v. 4.2. Users Manual. U.S. Geological Survey, Virginia, U.S.A (2006)

[8] Tanner, C.C., Clayton, J.S., Upsdell, M.P.: Effect of Loading Rate and Planting on Treatment of Daily Farm Wastewaters in Constructed Wetlands – I. Removal of Oxygen Demand, Suspended Solids and Faecal Coliforms. Water Research 29, 17-26 (1995)

[9] Anderson, M.P.: Heat as a Ground Water Tracer. Groundwater 43, 951-968 (2005)

Further Results of Mean-value Type in $\mathbb{C}$ and $\mathbb{R}$

Lubomir Markov

It is a well-known fact of classical analysis that a direct extension of Rolle's Theorem does not hold for complex functions: $f(z) = \exp(2\pi iz) - 1$ has the property $f(0) = f(1) = 0$, but $f'(z) \neq 0,\ \forall z$. In 1992, Evard and Jafari [2] published an interesting complex Rolle's theorem which asserts that the zeros of $\Re(f')$ and $\Im(f')$ separate the zeros of a holomorphic function $f(z)$ along the line segments connecting pairs of zeros. In a recent work [4] (presented at the 2014 conference "Math Days in Sofia"), we extended the Evard-Jafari theorem in the following direction:

Theorem 1 *Theorem 1 (Sharper Evard-Jafari Theorem) Let $f(z) = u(z) + iv(z)$ be holomorphic on the open convex set $D_f \subseteq \mathbb{C}$ and let $A, B \in D_f$ be such that $f(A) = 0 = f(B)$. Suppose $A = a_1 + ia_2,\ B = b_1 + ib_2$ and define the real functions*

$$\begin{aligned} \phi(t) &= (b_1 - a_1)u(A + t(B - A)) + (b_2 - a_2)v(A + t(B - A)), \\ \psi(t) &= (b_1 - a_1)v(A + t(B - A)) - (b_2 - a_2)u(A + t(B - A)), \qquad t \in [0, 1]. \end{aligned}$$

Suppose $0 = \tau_0 < \tau_1 < \cdots < \tau_m = 1$ $(m \geq 1)$ are zeros of $\phi(t)$, with corresponding points $P_j = A + \tau_j(B - A),\ j = 0, \cdots, m - 1$ on the segment $[A, B]$. Consider each interval (τ_j, τ_{j+1}) and each subsegment (P_j, P_{j+1}). If $\phi(t) \neq 0,\ t \in (\tau_j, \tau_{j+1})$, then there will be an odd number of points $z_{1,j} \cdots, z_{q,j} \in (P_j, P_{j+1})$ such that $\Re\big[f'(z_{1,j})\big] = 0, \cdots, \Re\big[f'(z_{q,j})\big] = 0$ (if it is not known that $\phi(t) \neq 0$ for $t \in (\tau_j, \tau_{j+1})$, there will be at least one such point). A similar property holds for $\psi(t)$.

Another result obtained in [4] concerns Flett's Mean Value Theorem [3] and its extensions [1] in $\mathbb{R}$ and $\mathbb{C}$. For $\alpha, \beta \in \mathbb{C}$, define $\langle \alpha, \beta \rangle = \Re\big(\alpha\bar{\beta}\big)$. Theorem 2 in [1] is:

Theorem 2 *The Davitt-Powers-Riedel-Sahoo Mean Value Theorem Let $D_f \subset \mathbb{C}$ be open and convex, $f : D_f \to \mathbb{C}$ - holomorphic, $A, B \in D_f$. Then $\exists\, z_1, z_2 \in (A, B)$ such that*

$$\begin{aligned} \Re\big[f'(z_1)\big] &= \frac{\Big\langle B - A, f(z_1) - f(A)\Big\rangle}{\big\langle B - A, z_1 - A\big\rangle} + \frac{1}{2}\frac{\Re\big[f'(B) - f'(A)\big]}{B - A}(z_1 - A), \\ \Im\big[f'(z_2)\big] &= \frac{\Big\langle B - A, -i\big[f(z_2) - f(A)\big]\Big\rangle}{\big\langle B - A, z_2 - A\big\rangle} + \frac{1}{2}\frac{\Im\big[f'(B) - f'(A)\big]}{B - A}(z_2 - A). \end{aligned}$$

We proved a better version of the theorem (see [4]):

Theorem 3 *Let $f(z) = u(z) + iv(z)$ be holomorphic on the open convex set $D_f \subseteq \mathbb{C}$ and let $A = a_1 + ia_2 \in D_f$, $B = b_1 + ib_2 \in D_f$. Then $\exists\, z_1, z_2 \in (A, B)$ such that*

$$\Re\big[f'(z_1)\big] = \Re\left[\frac{f(z_1) - f(A)}{z_1 - A} + \frac{1}{2}\frac{f'(B) - f'(A)}{B - A}(z_1 - A)\right],$$

$$\Im\big[f'(z_2)\big] = \Im\left[\frac{f(z_2) - f(A)}{z_2 - A} + \frac{1}{2}\frac{f'(B) - f'(A)}{B - A}(z_2 - A)\right].$$

The purpose of the present paper is to continue with the investigation initiated in [4] and to establish a few other theorems of mean-value type which are believed to be new.

Key words and phases: Rolle's Theorem, Evard-Jafari Theorem, Mean Value Theorems in the complex domain, Flett's Mean Value Theorem, Davitt-Powers-Riedel-Sahoo Theorem.

References

[1] R. Davitt, R. Powers, T. Riedel and P. Sahoo, Flett's Mean Value Theorem for Holomorphic Functions *Math. Magazine* **72** (1999), 304-307.

[2] J. - Cl. Evard and F. Jafari, A Complex Rolle's Theorem, *Amer. Math. Monthly* **99** (1992), 858-861.

[3] T.M. Flett, A Mean Value Theorem, *Math. Gazette* **42** (1958), 38-39.

[4] L. Markov, Mean Value Theorems for Analytic Functions, *Serdica Math J.* **41** (2015).

Computer Aided Modeling of Ultrasonic Surface Waves Propagation in Materials with Gradient of the Properties

Todor Partalin, Yonka Ivanova

The propagation of ultrasonic waves depends on physical properties of the medium, like the volume density, elastic moduli and Poisson's ratio [1, 3]. In the materials with internal stresses these properties change due to deformations caused by stresses. The differencies of the chemical composition or phase structure have similar effect. Dispersion of surface ultrasonic wave occurs as a result of heterogeneity of the media produced by some of mentioned reasons. The investigations related to the ultrasonic Rayleigh waves in nonuniform media provide opportunities for evaluation of the physical and mechanical properties in the surface and subsurface layers of materials as well as stress analysis in metal structures [2, 3, 4].

The present work deals with computer modeling of generation, propagation and receiving of the ultrasonic Rayleigh impulse in material with properties' gradient. The spectrum of an ultrasonic signal, having passed through a material, is determined by the spectrum of the exciting electrical signal, frequency characteristics of the transmitting and receiving transducers and by the material characteristics. The dispersion of the Rayleigh wave is simulated by spectral decomposition of impulse and processing components considering wave penetration and wave velocity changes caused by gradient of the mechanical characteristics. Simulated ultrasonic waveforms allow evaluation of the time delay effect induced by stress gradient. Application of ultrasonic wave for stress state analyses is possible on the basis of spectral analysis and phase comparisons of ultrasonic impulse.

Acknowledgements: The research is performed as a part of project 147/2015 with Sofia University "St. Kliment Ohridski".

References

[1] Nondestructive testing, Handbook, Vol. 4, Moscow, Publ. House "Spectr" (2007) (in Russian).

[2] Hirao, M., Fukuoka, H., Hori, K.,. Acoustoelastic effect of Rayleigh surface wave in isotropic material. ASME J. Appl. Mech. 1981, Vol. 48, pp. 119-124.

[3] Chernoochenko, F. G. Makhort, and O. I. Gushcha, Use of the theory of acoustoelasticity of Rayleigh waves to determine stresses in solids, Int. Applied Mechanics, vol. 27, pp. 38-42, 1991.

[4] Med.O.Si-Chaib, H. Djelouah, T. Boutkedjirt, An ultrasound method for the acoustoelastic evaluation of simple bending stresses. NDT&Intern.34 (2001) 521-529.

InterCriteria Analysis of Simple Genetic Algorithms Performance

Tania Pencheva, Maria Angelova

Aim: Recently developed InterCriteria Analysis is here applied to assess the performance of simple genetic algorithms for the purposes of a parameter identification of a fermentation process.
Methods: InterCriteria Analysis (ICA) approach employs the apparatuses of index matrices and intuitionistic fuzzy sets. ICA works based on an existing index matrix with multiobject multicriteria evaluations aiming to produce a new index matrix that contains intuitionistic fuzzy pairs with the correlations revealed to exist in between the set of evaluation criteria. In this investigation ICA is implemented to assess the performance of simple genetic algorithms and to determine possible dependencies between some criteria preliminary defined as of significant importance.
Simple genetic algorithms (SGA) as representatives of the biologically-inspired ones, are chosen to be in the focus of this investigation. SGA are promising stochastic technique since they have been proven as quite successful in solving of many problems in the field of complex dynamic systems optimization. Standard SGA searches a global optimal solution using three main genetic operators in a sequence selection, crossover and mutation. Having in mind that the basic idea of genetic algorithms is to imitate the processes in living nature (i.e. mechanics of natural selection and genetics), one can assume that the probability of mutation to take place firstly, following by crossover, is comparable to the probability that both processes to occur in a reverse order; or, selection to be performed after crossover and mutation, no matter of their order. Following that idea, altogether six modifications of standard SGA, concerning the sequence of execution of three main genetic operators, have been developed aiming to improve model accuracy and algorithm convergence time.
Object: In this investigation SGA are applied for such a challenging problem as a parameter identification of a fed-batch fermentation process. Yeast *Saccharomyces cerevisiae* have been chosen as they appear as microorganisms with numerous applications in food and pharmaceutical industries and have been also widely used as model organisms in genetic engineering and cell biology due to their well known metabolic pathways.
Results and discussion: Results obtained from the application of altogether six kinds of SGA for the purposes of parameter identification of *Saccharomyces cerevisiae* fed-batch fermentation process have been thoroughly analysed implementing ICA approach. Degrees of agreement and disagreement between preliminary determined criteria – algorithms outcomes (i.e. model accuracy and convergence time), from the one hand, and model parameters estimations, and from the other hand, have been established. This is going to lead to an additional exploring of the model itself and the relation between models parameters and optimization algorithm outcomes, which will be valuable especially in the case of modelling of living systems, such as fermentation processes.

Statics of Particles: Interval Arithmetic Approach

Evgenija D. Popova

Statics is the study of methods for quantifying the forces between bodies [1]. Forces are responsible for maintaining balance and causing motion of bodies, or changes in their shape. Statics is an essential prerequisite for many branches of engineering, such as mechanical, civil, aeronautical, bioengineering, robotics, and others that address the various consequences of forces. Societal concerns have led to more stringent requirements for the safety and reliability of products; they demand new methods for validation, verification, and the quantification of uncertainties, [2].
In this work we consider force equilibrium equations where forces are considered as uncertain and their magnitude varies within given real compact intervals. The goal is to determine the best interval estimation for some unknown forces and/or reactions which are also uncertain. This is a difficult challenging task since the classical interval arithmetic [4] does not posses group properties and, therefore, it is not suitable for modeling interval equilibrium equations.
Proposed is an interval model where the uncertain (interval) forces are defined in a simple and unique way. An efficient computational procedure, based on the algebraic properties of the complete algebraic structure of proper and improper intervals [3], is proven to deliver the best interval enclosure for the magnitude of the unknown forces and/or reactions involved in the interval equilibrium equations together with the corresponding direction of the force (reaction). Various practical examples illustrate the application of the proposed methodology and the various sources of uncertainty. The same approach is applicable also to other interval equilibrium equations.

References

[1] Beer, F.P., Johnston, E.R., Mazurek, D.F., Cornwell, P.J., Eisenberg, E.R., Vector Mechanics for Engineers: Statics and Dynamics, 9th edition, McGraw-Hill, 2010.

[2] A forward look: Mathematics and Industry, European Science Foundation, 2011.

[3] Kaucher E. (1980) Interval analysis in the extended interval space IR. Computing Suppl. 2:33-49.

[4] Moore R.E., Kearfott R.B., Cloud M.J. (2009) Introduction to Interval Analysis, SIAM Press, Philadelphia.

Emergence of Drug Resistance in Cancer from the Perspective of Environmental Competition

Peter Rashkov

A major obstacle in chemotherapeutical cure of a tumour is the emergence of drug-resistant clones inside the tumour, an event which ultimately leads to tumour relapse and poor patient prognosis. Despite much experimental and clinical effort, the mechanisms behind acquisition of drug resistance in cancers are still poorly understood.
A recent experimental study [1] reports that targeted therapy of mixed tumours consisting of both sensitive and resistant clones leads to an accelerated proliferation of resistant clones compared to vehicle treatment. The authors propose that this ensues from a stress response of the drug-sensitive clones which release signalling macromolecules into the tumour microenvironment that support and stimulate the expansion of the drug-resistant clones.
I propose a mathematical model based on environmental competition to demonstrate that accelerated proliferation of the drug-resistant clones can occur independently of any additional signalling. Thus, it is possible for the volume of resistant clones to expand faster under treatment in a mixed tumour (relative to vehicle). This paradox happens even when the resistant clones are at a proliferative disadvantage compared to the sensitive clones. The model predicts, furthermore, that under certain conditions the resistant clones inside a mixed tumour under targeted therapy, in fact, can grow faster than those originating from a fully resistant tumour.
The model is based on a reaction-diffusion system with a nonlinear diffusion term. Travelling wave solutions of the model are studied analytically and numericaly. The model raises attention to the role of tumour spatial structure and organisation, which is often omitted from experimental and evolutionary models of cancer [2].

References

[1] Obenauf, A. C., and Coauthors, 2015: Therapy-induced tumour secretomes promote resistance and tumour progression. *Nature*, **520**, 368–372.

[2] Korolev, K., J. B. Xavier, and J. Gore, 2014: Turning ecology and evolution against cancer. *Nature Rev. Cancer*, **14**, 371–380.

InterCriteria Analysis of Relations between Model Parameters Estimates and ACO Performance

Olympia Roeva, Stefka Fidanova

In this paper we applied the approach InterCriteria Analysis (ICA) to establish the existing relations and dependencies of defined parameters in non-linear model of an *E. coli* fed-batch cultivation process. Moreover, based on results of series of Ant Colony Optimizatpon (ACO) identification procedures we observed the mutual relations between model parameters and ACO outcomes, such as execution time and objective function value.

The ICA is developed with the aim to gain additional insight into the nature of the criteria involved and discover on this basis existing relations between the criteria themselves. It is based on the apparatus of the Index Matrices (IM) and the Intuitionistic Fuzzy Sets. The ICA can be applied for decision making in different areas of science and practice.

In the case of modelling of cultivation processes ICA approach could be very useful. Cultivation processes are characterized with complex, non-linear dynamic and their modelling is a hard combinatorial optimization problem. The parameter identification is of key importance for modelling process and additional knowledge about the model parameters relations will be extremely useful to improve the model accuracy. The use of meta-heuristic techniques such as ACO has received more and more attention. This techniques offer good solutions, even global optima, within reasonable computing time, so we choose to use ACO for estimation of the model parameters.

We performed a series of model identification procedures applying ACO. To estimate the model parameters we applied consistently 11 differently tuned ACO. We used various population sizes – from 5 to 100 ants in the population.

In terms of ICA we defined five criteria, namely model parameters (maximum specific growth rate, μ_{max}; saturation constant, k_S and yield coefficient, $Y_{S/X}$) and ACO outcomes (execution time, T and objective function value, J). Based on ICA we examined the obtained parameters estimates and discussed the conclusions about existing relations and dependencies between defined criteria.

Following the ICA theory a pseudocode of the algorithm used in this study for calculating the "degrees of agreement" and "degrees of disagreement" between two criteria C and C' is presented below.

Based on the presented **Algorithm 1** the ICA is implemented in the Matlab 7.5 environment. We obtain IMs that determine the degrees of "agreement" ($\mu_{C,C'}$) and "disagreement" ($\nu_{C,C'}$) between criteria for the three cases: (i) case of average results, (ii) case of worst results and (iii) case of best results.

The results show that the pairs of the considered model parameters and ACO outcomes (defined five criteria, ten pairs) could grouped as follows:

- criteria pairs that are in negative consonance;
- criteria pairs that are in dissonance;

Algorithm 1 Calculating "agreement" and "disagreement" between two criteria

Require: Vectors $\hat{V}(C)$ and $\hat{V}(C')$

function DEGREE OF AGREEMENT($\hat{V}(C), \hat{V}(C')$)
  $V \leftarrow \hat{V}(C) - \hat{V}(C')$
  $\mu_{C,C'} \leftarrow 0$
  for $i \leftarrow 1$ to $\frac{n(n-1)}{2}$ **do**
    if $V_i = 0$ **then**
      $\mu_{C,C'} \leftarrow \mu_{C,C'} + 1$
    end if
  end for
  $\mu_{C,C'} \leftarrow \frac{2}{n(n-1)} \mu_{C,C'}$
  return $\mu_{C,C'}$
end function

function DEGREE OF DISAGREEMENT($\hat{V}(C), \hat{V}(C')$)
  $V \leftarrow \hat{V}(C) - \hat{V}(C')$
  $\nu_{C,C'} \leftarrow 0$
  for $i \leftarrow 1$ to $\frac{n(n-1)}{2}$ **do**
    if abs$(V_i) = 2$ **then** ▷ abs: absolute value
      $\nu_{C,C'} \leftarrow \nu_{C,C'} + 1$
    end if
  end for
  $\nu_{C,C'} \leftarrow \frac{2}{n(n-1)} \nu_{C,C'}$
  return $\nu_{C,C'}$
end function

- criteria pairs that are in positive consonance.

Due to stochastic nature of ACO we observed some different criteria dependences in the three cases – case of worst, best and average results. Obtained here results are compared with the ICA results achieved using Genetic Algorithms (GA) as optimization techniques. Thus, based on the results using ACO and GA and on the worst, best and average estimates of each optimization techniques we defined more precisely the given criteria pair in which group (negative consonance, dissonance or positive consonance) falls.

Newtonian and Non-Newtonian Pulsatile Blood Flow In Arteries with Model Aneurysms

Sonia Tabakova, Nikola Nikolov, Plamen Rajnov, Stefan Radev

The cardiovascular diseases depend directly on the blood flow dynamics. The in vivo measurement techniques is unable to resolve the phenomena in a living human body. Thus the mathematical modeling and numerical simulations are expected to play an important role in this case using different hemorheological models to predict, for example, the genesis of the atherosclerosis and the formation and rupture of the aneurysms.

The blood is a suspension of particles and plasma, which has a non-Newtonian character as a fluid. It is a typical representative of the shear thinning fluids with an apparent viscosity dependent on the shear rate. Several non-Newtonian rheological models are used to express the blood rheology: the Carreau model, the Casson model, the Power law model and others [1]. Some of these models, such as that of Carreau, give a non-linear dependence of the shear stress on the shear rate. The proper knowledge of the viscosity leads to a proper knowledge of the Wall Shear Stresses (WSS), which are of a major importance for the prediction of an aneurism rupture. The problem becomes more complicated if the pulsatile character of the blood flow is considered.

In the present work the numerical solutions for the oscillatory flow velocity due to the Newtonian and Carreau model are constructed analytically and numerically for a straight long tube and for a tube (artery) with a model aneurysm [2]. The numerical solutions are obtained by the finite-difference method (FDM) for the straight tube and using the software ANSYS/FLUENT for both models. The numerical results obtained by ANSYS/FLUENT for the velocity in a straight long tube are validated by the analytical and numerical solutions using the FDM for the Newtonian and Carreau models [3] for different Womersley numbers [4], correspondent to different tube radii. The comparisons between the velocities and between the WSS found by the Newtonian model and by the Carreau model for the straight long tube show a decrease when increasing the Womersley number, i.e., increasing the tube radius. The obtained peak WSS for the human carotid are within the experimental ranges [5]. The obtained peak WSS from the oscillatory flow in a straight long tube are lower than those in a tube with model aneurysm, which can be used as an indicator for further clinical examinations.

Acknowledgment The authors have been partially supported for this research by the National Science Fund of Bulgarian Ministry of Education and Research: Grant DFNI-I02/3.

References

[1] T. G. Myers, *Phys. Review E* **72**, 066302 (2005).

[2] S. S. Gopalakrishnan, B. Pier and A. Biesheuvel, *Journal Fluid Mechanics*, **758**, 150–179 (2014).

[3] S. Tabakova, E. Nikolova and St. Radev *AIP conference proceedings*, **1629**, 336–343 (2014).

[4] J. R. Womersley, *The Journal of Physiology* **127**, 553–563 (1955).

[5] R. S. Reneman and A. P. G. Hoeks, *Med Biol Eng Comput* **46**, 499–507 (2008).

Reduced Rule Base Fuzzy-Neural Networks

Margarita Terziyska, Yancho Todorov

Neural Networks and Fuzzy Logic systems are well known as universal approximators and they are successfully used for modeling and identification of complex dynamical systems. Hybrid Neuro-Fuzzy Networks emerged as a synergism of these two major directions in computational intelligence. They possess the learning capabilities similar to those of neural networks, and provide the interpretability and "transparency" of results, inherent to the fuzzy approach. In this paper are presented two different neuro-fuzzy systems with reduced rules bases. A great motivation for this research is to propose potential solutions able to avoid some of the disadvantages of the classical neuro-fuzzy systems, as the great number of updated parameters, needed to represent a complex nonlinear behavior and the associated computational time to perform the algorithm execution. Both proposed models are realized as a Distributed Adaptive Neuro-Fuzzy Architecture (DANFA), where the input space is distributed along a set of fuzzy inferences and a Semi-Fuzzy Neural Network (SFNN), with selective fuzzification of the input space. As inference mechanism, a classical Takagi-Sugeno approach is employed. The strengthen the robustness and the nonlinear approximation properties of the models, a set of Gaussian membership functions along each model input is considered. As a learning procedure for the designed structures, a simplified two-step gradient algorithm based on minimization of an instant quadratic error measurement function is applied. Thus, in each sampling period of a model operation, two groups of parameters are being scheduled: the premise - the parameters of the fuzzy membership functions and the consequent - the parameters of the liner modeling functions. Applying the proposed principles lead to reduction of the both associated fuzzy rule's premise and consequent parameters. This facilitates the on-line learning procedure and reduce the computational effort without a great loss of modeling accuracy. To demonstrate the potentials of the proposed networks, simulation experiments with two benchmark chaotic time systems - Mackey-Glass and Rossler are studied. They produce fast changing by amplitude and frequency signals which often are hard to be modeled in real time. The obtained results show accurate models performance with minimal modeling error. Thus, their application areas may be extended to modeling of fast changing plant processes and process control in the framework of model based control.

Accuracy Assessment of Linear Craniometric Measurements on a Laser Scanning Created 3D Model of a Dry Skull

Diana Toneva, Silviya Nikolova, Ivan Georgiev, Assen Tchorbadjieff

The laser scanning is a method of capturing surface data from real objects using laser technology. The collected data could be used for creating 3D digital models. The high resolution images created by 3D laser scanning have increasing application in physical anthropology in the last years. Although the usage of laser scanners reproduces only the outer surface of the scanned object without capturing its internal structure, it is very useful for digitizing bone samples because of its portability, easy manipulating with digital models and reduced risk of damage of the real objects (Bibliowicz et al., 2011). The 3D digital models can be used for metrical and macroscopical analyses, visualization, virtual archiving and conservation, making 3D printed copies, etc. The metric characterization of the bones is an important part of the anthropological investigation of human bone remains. Craniometry represents quantitative characteristic of the skull. It is performed by measuring of the distances between definite landmarks of the skull. Most of the measurements represent linear dimensions on different anatomical structures. However, 3D digital models contribute to more easily calculating on the computer of hard to measure bone characteristics, such as volume, surface area, and surface curvatures (Bibliowicz et al., 2011).
The aim of this study was to compare the accuracy of the directly taken linear measurements of a skull with corresponding measurements of the 3D model created by laser scanning. For that purpose a skull from the osteological collection at the Institute of Experimental Morphology, Pathology and Anthropology with Museum, Bulgarian Academy of Sciences was scanned using laser scanner Creaform VIUscan^{TM} and a 3D model was created. The comparison in the study was performed between thirteen craniometric measurements. The conventional ones were taken with standard sliding and spreading calipers. The 3D model could measure using MeshLab and Geomagic Verify Viewer. Both skull and 3D model were measured by two examiners. Inter-examiner and intra-examiner reliability was calculated. The measurements obtained from the 3D model and the directly taken ones were comparable and accurate. The evaluation of the accuracy between both methods is of great importance, since the skull measurements have been used in sex determination, race investigations, identification of unknown bone remains, etc.

References

[1] Bibliowicz J., Khan A., Agur A., Singh K., High-Precision Surface Reconstruction of Human Bones from Point-Sampled Data, ISHS 2011 Conference Proceedings: International Summit on Human Simulation, 1-10, 2011.

Finite Difference Schemes for Fractional Oldroyd-B Fluids

Daniela Vasileva, Ivan Bazhlekov, Emilia Bazhlekova

Viscoelastic non-Newtonian fluids have broad application in industry (molten plastics, oils and greases, suspensions, emulsions, pulps, etc.). They are frequently modeled by linear constitutive equations which involve fractional derivatives [1, 3, 12]. Such models provide a higher level of adequacy than the classical integer-order models due to the nonlocal character of the fractional derivatives, leading to their ability to describe more adequately phenomena with memory. Unlike the classical models which exhibit exponential relaxations, the fractional models show power-law behaviors which are widely observed in a variety of experiments [9]. On the other hand, the same nonlocality property of the fractional derivatives complicates the design of fast and accurate numerical techniques for the corresponding fractional order differential equations.

We consider the following Rayleigh-Stokes problem for a generalized Oldroyd-B fluid (see [3, 12] for details on the derivation):

$$(1 + aD_t^\alpha)u_t = \mu(1 + bD_t^\beta)\Delta u + F(x, y, t), \quad (x, y) \in (0, 1)^2, \ t > 0, \tag{1}$$

$$u(x, y, 0) = u_t(x, y, 0) = 0, \quad (x, y) \in [0, 1]^2, \tag{2}$$

$$u(x, y, t) = v(x, y, t), \quad t > 0, \ x = 0 \text{ or } x = 1 \text{ or } y = 0 \text{ or } y = 1. \tag{3}$$

Here $u(x, y, t)$ is the unknown velocity field of a unidirectional flow (in the z-direction), $a, b \geq 0$, $\mu > 0$, D_t^α and D_t^β are Riemann-Liouville fractional time derivatives of orders $\alpha \in (0, 1)$ and $\beta \in (0, 1)$.

Analytical solutions to this problem are derived in the form of eigenfunction expansions e.g. in [3, 12, 2], to mention only few of many recent publications. However, numerical studies of problem (1)-(3) are scarce, especially in the general case $a \neq 0$ and $b \neq 0$ [11].

Essential part of a numerical algorithm for problem (1)-(3) is the discretization of the fractional derivatives in time. Reviews of the different discretization techniques can be found in [7, 8, 5, 4].

The so-called $L1$ and $L2$ approximations are introduced in [7]. The $L1$ scheme is suitable to approximate the fractional derivative D_t^α for $\alpha \in (0, 1)$ with order of convergence $O(\tau^{2-\alpha})$, where τ is the time step. The $L2$ scheme approximates the fractional derivative of order $\alpha \in (1, 2)$ with convergence rate $O(\tau^{3-\alpha})$ (see [10]).

The first order Grünwald-Letnikov approximation and the second order Lubich approximation (see [6]) of the fractional time derivatives are also frequently used in the discretization of fractional equations.

Here we present several finite-difference schemes, using the above mentioned approximations of the fractional time derivatives and second or compact fourth order discretization in space. Extensive numerical experiments for different values of α and β are performed in order to illustrate the stability and convergence.

Acknowledgments. The work is partially supported by Grant DFNI-I02/9 from the Bulgarian National Science Fund.

References

[1] R. Bagley and P. Torvik. *J. Rheol.*, 30:133–155, 1986.

[2] E. Bazhlekova and I. Bazhlekov. *Fract. Calc. Appl. Anal.*, 17:954–976, 2014.

[3] C. Fetecau, M. Jamil, C. Fetacau, and D. Vieru. *Z. Angew. Math. Phys.*, 60:921–933, 2009.

[4] B. Jin, R. Lazarov, and Z. Zhou. Two fully discrete schemes for fractional diffusion and diffusion wave equations. (arxiv.org/pdf/1404.3800v3.pdf).

[5] C. Li and F. Zeng. *Int. J. Bifurcation Chaos*, 22:1230014 (28 p.), 2012.

[6] C. Lubich. *SIAM J. Math. Anal.*, 17:704–719, 1986.

[7] K. Oldham and J. Spanier. *The Fractional Calculus.* Academic Press, San Diego, CA, 1974.

[8] I. Podlubny. *Fractional Differential Equations.* Academic Press, San Diego, CA, 1999.

[9] D. Song and T. Jiang. *Rheol. Acta*, 37:512–517, 1998.

[10] Z. Sun and X. Wu. *Appl. Numer. Math.*, 56:193–209, 2006.

[11] D. Vasileva, I. Bazhlekov, and E. Bazhlekova. *AIP Conference Proceedings*, 1684:080001, 2015.

[12] C. Zhao and C. Yang. *Appl. Math. Comput.*, 211:502–509, 2009.

Equivalence of Models of Freeze-Drying

Milena Veneva, William Lee

Freeze-drying is a preservation process, consisting of two main stages: primary drying and secondary drying. The process is very popular in the food and pharmaceutical industries as a process which removes water (or solvents as a whole) from heat-sensitive products that will be damaged if a standard drying procedure is used instead. During the primary drying the material to be dried is frozen below its triple point, then the surrounding pressure is lowered, and enough heat is supplied to the material so as the water to sublimate. In this initial drying phase about 95% of the water in the material is sublimated. This phase may be slow (can be several days in industry), because if too much heat is added, the material's structure could be altered. The aim of the secondary drying stage of the process is to remove unfrozen water molecules, since the ice was removed in the primary drying phase. This part of the freeze-drying process is governed by the material's adsorption isotherms. In this phase the temperature is raised higher than in the primary drying phase so as to break any physico-chemical interactions that have formed between the water molecules and the frozen material. Usually the pressure is also lowered in this stage to encourage desorption.
In a typical phase diagram (see figure 1), the boundary between gas and liquid runs from the triple point to the critical point. Freeze-drying (blue arrow) brings the system around the triple point, avoiding the direct liquid-gas transition seen in ordinary drying time (green arrow).

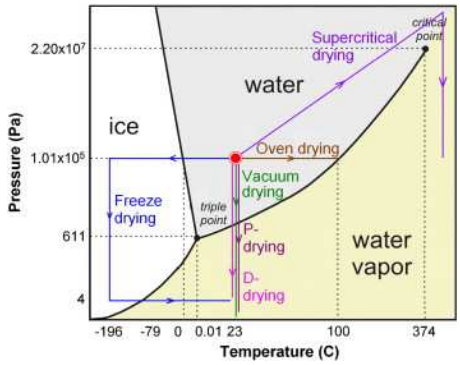

Figure 1: Diagram of freeze-drying (this picture was taken from http://freezedryinc.com (the link has been active as of 30.10.2015))

Two different one-dimensional models of secondary drying in a vial are built. The first one consists of coupled heat and mass balances equations:

$$\rho_e\, c_{p,e}\, \frac{\partial T}{\partial t} + c_{p,w}^{(g)}\, N_w \frac{\partial T}{\partial z} = \frac{\partial}{\partial z}\left(k_e \frac{\partial T}{\partial z}\right) + \triangle H_v\, \rho_s\, \frac{\partial c_{sw}}{\partial t};$$

$$\gamma \frac{\partial}{\partial t}\left(\frac{p_w}{T}\right) + \frac{\partial N_w}{\partial z} = -\rho_s \frac{\partial c_{sw}}{\partial t};$$

$$N_w = -\frac{M_w}{R_{un}\, T}\left(d_1 + d_2\, p_w\right) \frac{\partial p_w}{\partial z};$$

$$\frac{\partial c_{sw}}{\partial t} = -r_d\, c_{sw};$$

$$c_{sw} = c_{sw}^0,\ t = 0.$$

At the beginning of secondary drying the temperature, the water vapor pressure, and the concentration of bound water are known. These are taken as initial conditions of the system. On the top of the vial radiation heat flux and constant water vapor pressure are applied; at the bottom of the vial Newton's law of cooling and zero water vapor mass flux are considered.
On the other hand, the second model uses a modified Richards equation:

$$\frac{\partial \theta_v}{\partial t} = -\frac{\partial q_v}{\partial z} + S(H);$$

$$c_{p,e} \frac{\partial T}{\partial t} + \triangle H_v \frac{\partial \theta_v}{\partial t} = \frac{\partial}{\partial z}\left(\lambda \frac{\partial T}{\partial z}\right) - c_{p,w}^{(g)} \frac{\partial q_v\, T}{\partial z} - \triangle H_v \frac{\partial q_v}{\partial z};$$

$$q_v = -K_{vh} \frac{\partial H}{\partial z} - K_{vt} \frac{\partial T}{\partial z}.$$

The same initial and boundary conditions as the ones described above are applied to the second model.
Using scale transformations derived from the PDEs and the BCs, the first model is nondimensionalized. After an asymptotic reduction, this model is simplified even more. It is proven that the reduced model is equivalent to the model that uses the modified Richards equation if no air exists in the vials and in the chamber of the freeze-drier.
This result shows that there is an opportunity for technology transfer, since solvers developed for modelling groundwater flows using Richards equations can be also used to model the economically important problem of freeze-drying.

Key words: Freeze-drying, secondary drying, Richards equation, numerical analysis.

Comparing Bézier Curves and Surfaces for Coincidence

Krassimira Vlachkova

It is known that Bézier curves and surfaces may have multiple representations by different control polygons. The polygons may have different number of control points and may even be disjoint, see Fig. 1. This phenomenon causes difficulties in variety of applications where it is important to recognize cases where different representations define same curve (surface) or partially coincident curves (surfaces). The problem of finding whether two arbitrary polynomial curves are the same has been addressed in [1] where the curves are reduced into canonical irreducible forms using monomial basis, then they are compared and their shared domains, if any, are identified. Here we present an alternative geometric algorithm based on subdivision that compares two input control polygons and reports the coincidences between the corresponding curves if they are present. Our algorithm works in two phases as follows. In the first phase the control polygons are tested for reducibility. We adopt a set of routines from Mathematica package and transform the control polygons to an irreducible form which is unique for a properly parameterized Bézier curve as shown in [2]. In the second phase the obtained irreducible control polygons are checked for partial coincidence. We propose a new geometric approach based on subdivision. We generalize the algorithm for Bézier surfaces. The algorithms are implemented and tested using Mathematica package. The experimental results are presented and analysed.

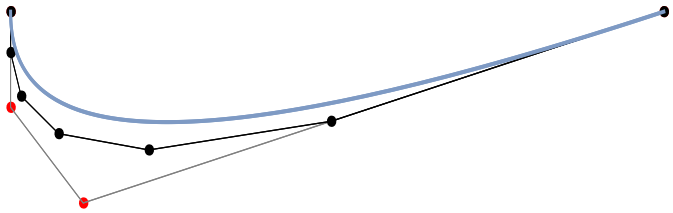

Figure 1: Cubic Bézier curve defined by two different polygons

Acknowledgments. This work was partially supported by the Bulgarian National Science Fund under Grant No. DFNI-T01/0001.

References

[1] Pekerman, D., Seong, J-K., Elber, G., Kim, M-S.: Are two curves the same?, Comput.-Aided Geom. Design and Appl., 2(1-4), 85-94 (2005)

[2] Sánchez-Reyes, J.: On the conditions for the coincidence of two cubic Bézier curves, J. of Comput. and Appl. Math., 236(6), 1675-1677 (2011)

Spectral Theory of $\mathrm{sl}(3,\mathrm{C})$ Auxiliary Linear Problem with $\mathbf{Z_2}\times\mathbf{Z_2}\times\mathbf{Z_2}$ Reduction of Mikhailov Type

Alexandar B. Yanovski

We consider an auxiliary system introduced recently, [1]:

$$L_{S_{\pm 1}}\psi = (i\partial_x + \lambda S_1(x) + \lambda^{-1}S_{-1}(x))\psi = 0. \tag{1}$$

In the above the "potential functions" $S_1(x)$ and $S_{-1}(x)$ are 3×3 traceless matrix functions. In addition, it is assumed that the set of the fundamental solutions of the above system should be invariant under a group generated by the following transformations:

$$\begin{array}{l} g_0(\psi)(x,\lambda) = \left[\psi(x,\lambda^*)^\dagger\right]^{-1} \\ g_1(\psi)(x,\lambda) = H_1\psi(x,-\lambda)H_1, \quad H_1 = diag(-1,1,1) \\ g_2(\psi)(x,\lambda) = H_2\psi(x,\frac{1}{\lambda})H_2, \qquad H_2 = diag(1,-1,1). \end{array} \tag{2}$$

where $diag(a_1,a_2,a_3)$ denotes a diagonal matrix with diagonal elements a_1,a_2,a_3, * denotes complex conjugation and † stands for Hermitian conjugation. The above elements define a Mikhailov Reduction Grouup, [2], and since g_i^2 for $i=0,1,2$ is equal to identity, the group is isomorphic to $\mathbf{Z_2}\times\mathbf{Z_2}\times\mathbf{Z_2}$. Imposing reduction group forces S_{-1} to be equal to $H_2S_1H_2$ and S_1 to be of the form

$$S_{-1} = \begin{pmatrix} 0 & -u & v \\ -u^* & 0 & 0 \\ v^* & 0 & 0 \end{pmatrix} \tag{3}$$

where $u(x)$ and $v(x)$ are complex-valued functions defined on the real line. We also assume that $|u|^2+|v|^2=1$. One can show that this condition ensures that the values of $S_1(x)$ and S_{-1} will be in the orbit of the element $J_0 = diag(1,0,-1)$ with respect to the adjoint action of the group $SU(3)$ in $i$su(3) where su(3) is the Lie algebra of $SU(3)$. Imposing $|u|^2+|v|^2=1$ is motivated by the fact that in this case the L-operator $L_{S_1} = i\partial_x + \lambda S_1(x)$ could be regarded as a generalization of a pole gauge Generalized Zakharov-Shabat system on $\mathrm{sl}(3,\mathbf{C})$ which permits to develop the whole theory for it from the cases already studied [3]. We consider the system $L_{S_{\pm 1}}$ on the condition that $u(x)$ and $v(x)$ tend sufficiently fast to constant values u_0, v_0 when $x\to\pm\infty$ in the general situation when both $u_0, v_0 \neq 0$. The study of the spectral theory of this system (that is the study of its fundamental solutions and how the reductions (2) affect them) has been started in [1] where the degenerate cases $u_0=0$ and $v_0=0$ have been studied. In a conference talk GIQ, Varna, 2015 (to appear) we reported some results about the general case. This case is more involved than the degenerate one. Indeed, considering the asymptotic behavior of the fundamental solutions for $|x|\to\infty$ one sees that behave as $(\exp iJ(\lambda)x)A$ where $A=A(\lambda)$ is a matrix that does not depend on x and $J(\lambda) = (\lambda S_1 + \lambda^{-1}S_{-1})|_{u=u_0,v=v_0}$. For the construction and the study of the integral equations satisfied by the fundamental

analytic solutions (FAS) it is important to diagonalize $J(\lambda)$ and one easily finds that it has eigenvalues $0, \pm\mu$ where μ is a solution of the equation

$$\mu^2 = 2(|v_0|^2 - |u_0|^2) + (\lambda^2 + \lambda^{-2}). \tag{4}$$

In the degenerate case the r.h.s. is a square of a rational function but in the non-degenerate case it is not and so we are led to the study of the analytic properties of the branches of the square root $\mu(\lambda)$ of the r.h.s. of (4). Consequently, the analytic properties of the fundamental solutions depend on $\mu(\lambda)$ and we should study their behavior under the involutions of the extended complex plane

$$\varphi_1(\lambda) = \lambda^*, \quad \varphi_2(\lambda) = -\lambda, \quad \varphi_3(\lambda) = \lambda^{-1}. \tag{5}$$

We reported about this approach in the conference talk GIQ, Varna 2015 (to appear). However, there is one serious difficulty here and it is that in order to study the regular branches of $\mu(\lambda)$ one must make cuts in the complex plane and the analytic continuation of $\mu(\lambda)$ depends on the choice of these cuts. This makes the whole construction of the FAS depending on the cuts. In the present talk we explore another route. We are trying to formulate everything – fundamental solutions, scattering data, etc. etc. in the terms of the Riemann surface that corresponds to (4). It is a covering of the extended plane and has two points over $\lambda = 0$ and $\lambda = \infty$. The involutions (5) define involutions of this surface and naturally act on the fundamental solutions and the scattering data. We believe that such formulation is free from the flaws that involve selecting regular branches and will be more useful in the future.

References

[1] Gerdjikov V., Mikhailov A. and Valchev T., J. Phys. A: Math. Gen. **43** (2010).

[2] Mikhailov A., Physica **3D**, 3–117 (1981).

[3] Yanovski, A., J. Phys.: Conf. Ser. 621 012017 (2015).

Numerical Simulation of Nano-Indentation of Systems Containing Piezoelectric Material Layer

Roussislava Zaharieva, Dimitar Iankov, Roumen Iankov, Maria Datcheva

A robust finite element model is created for simulating nano-indentation of piezoelectric bulk materials and of systems comprising a piezoelectric coating and a non-piezoelectric substrate. The aim is to investigate the influence of different boundary conditions, finite element discretization, and the size of the geometrical model. The results obtained by the numerical simulation are compared against experimental data for systems of piezoelectric zirconate titanate (PZT) coating and silica substrates, as well as results obtained from conventional approach in nano-indentation data processing employing linear elasticity and not accounting for piezoelectric phenomena. An optimization procedure is employed to calibrate the material parameters through back analysis.

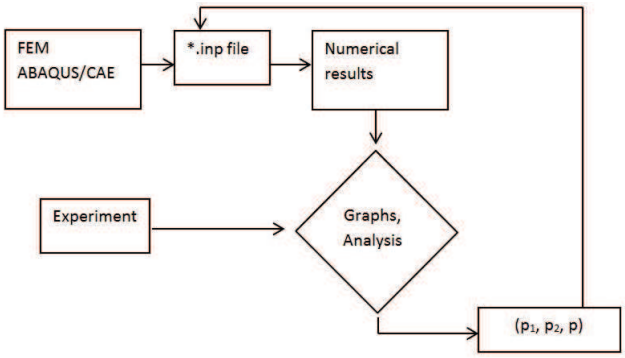

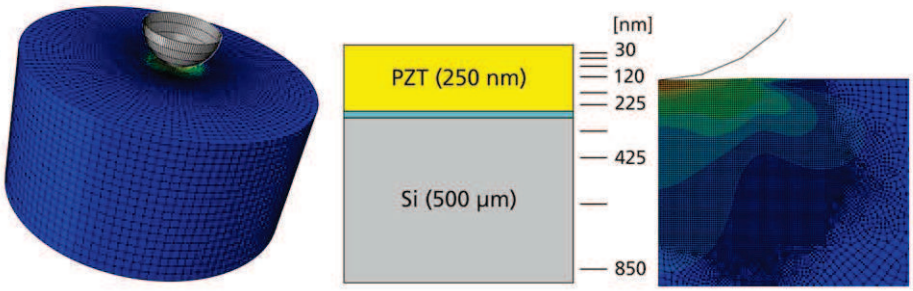

Part B

List of participants

Vassil Alexandrov
ICREA-BSC
Carrer Jordi Girona 29
8034 Barcelona, Spain
vassil.alexandrov@bsc.es

Andrey Andreev
Technical University of Gabrovo
Hadji Dimitar str. 4
5300 Gabrovo, Bulgaria
andreev@tugab.bg

Maria Angelova
Institute of Biophysics and
Biomedical Engineering
Bulgarian Academy of Sciences
105 Acad G. Bonchev Str.
1113 Sofia, Bulgaria
maria.angelova@biomed.bas.bg

Emanouil Atanassov
Institute of Information and
Communication Technologies
Bulgarian Academy of Sciences
Acad. G. Bontchev str., bl. 25A
1113 Sofia, Bulgaria
emanouil@parallel.bas.bg

Krassimir Atanassov
Institute of Biophysics and
Biomedical Engineering
Bulgarian Academy of Sciences
Acad. G. Bontchev str., bl. 105
1113 Sofia, Bulgaria
k.t.atanassov@gmail.com

Aleksey Balabanov
Institute of Information and
Communication Technologies
Bulgarian Academy of Sciences
Acad. G. Bontchev str., bl. 2
1113 Sofia, Bulgaria
alexey.balabanov83@gmail.com

Ivan Bazhlekov
Institute of Mathematics and Informatics
Bulgarian Academy of Sciences
Acad. G. Bonchev Str., Bl. 8
1113 Sofia, Bulgaria
i.bazhlekov@math.bas.bg

Emilia Bazhlekova
Institute of Mathematics and Informatics
Bulgarian Academy of Sciences
Acad. G. Bonchev Str., Bl. 8
1113 Sofia, Bulgaria
e.bazhlekova@math.bas.bg

Gergana Bencheva
Institute of Information and
Communication Technologies
Bulgarian Academy of Sciences
Acad. G. Bonchev Str., bl. 25A
1113 Sofia, Bulgaria
gery@parallel.bas.bg

Danail S. Brezov
Department of Mathematics
University of Architecture,
Civil Engineering and Geodesy
1 Hristo Smirnenski Blvd.
Sofia 1046, Bulgaria
danail.brezov@gmail.com

Alan Compelli
School of Mathematical Sciences
Dublin Institute of Technology
Kevin Street, Dublin 8
IRELAND
alan.compelli@mydit.ie

Maria Datcheva
Institute of Mechanics
Bulgarian Academy of Sciences
Acad. G. Bontchev St., bl. 4
1113 Sofia, Bulgaria
datcheva@imbm.bas.bg

Nina Dobrinkova
Institute of Information and
Communication Technologies
Bulgarian Academy of Sciences
Acad. G. Bontchev str., bl. 2
1113 Sofia, Bulgaria
ninabox2002@gmail.com
nido@math.bas.bg

O. Esquivel-Flores
IUNAM, Mexico and
Barcelona Supercomputing Centre
C/ Jordi Girona 29,
08034, Barcelona, SpainSpain

Wolfgang Fenz
Research Unit Medical Informatics
RISC Software GmbH
Johannes Kepler University Linz
Softwarepark 35
4232 Hagenberg, Austria
wolfgang.fenz@risc.uni-linz.ac.at

Stefka Fidanova
Institute of Information and
Communication Technologies
Bulgarian Academy of Sciences
Acad. G. Bonchev str., bl. 25A
1113 Sofia, Bulgaria
stefka@parallel.bas.bg

Dobromir Georgiev
Institute of Information and
Communication Technologies
Bulgarian Academy of Sciences
Acad. G. Bontchev str., bl. 25A
1113 Sofia, Bulgaria
dobromir@parallel.bas.bg

Ivan Georgiev
Institute of Information and
Communication Technologies
Bulgarian Academy of Sciences
Acad. G. Bontchev str., bl. 25A
1113 Sofia, Bulgaria
ivan.georgiev@parallel.bas.bg
and
Institute of Mathematics and Informatics
Bulgarian Academy of Sciences
Acad. G. Bonchev str., bl. 8
1113 Sofia, Bulgaria
ivan.georgiev@math.bas.bg

Krassimir Georgiev
Institute of Informatrion and
Communication Technologies
Bulgarian Academy of Science
Acad. G. Bontchev str., bl. 25A
1113 Sofia, Bulgaria
georgiev@parallel.bas.bg

Vanya Georgieva
Department of Neurosurgery
University Hospital "Sofiamed"
16 G.M. Dimitrov blv.
Sofia 1797, Bulgaria
docvania@abv.bg

Vladimir S. Gerdjikov
Institute of Nuclear Research and Nuclear
Energy,
Bulgarian Academy of Sciences,
72 Tsarigradsko chausee, Sofia 1784, Bulgaria,
gerjikov@inrne.bas.bg

Todor Gurov
Institute of Information and
Communication Technologies
Bulgarian Academy of Sciences
Acad. G. Bontchev str., bl. 25A
1113 Sofia, Bulgaria
gurov@parallel.bas.bg

Stanislav Harizanov
Institute of Information and
Communication Technologies
Bulgarian Academy of Sciences
Acad. G. Bonchev Str., bl. 25A
1113 Sofia, Bulgaria
sharizanov@parallel.bas.bg

Qingguo Hong
RICAM
Austrian Academy of Sciences
Altenberger Strasse 69
4040 Linz, Austria
hongqingguo1020@163.com

Ivan Hristov
Faculty of Mathematics and Informatics
St. Kliment Ohridski University of Sofia
5 James Bourchier Blvd.
1164 Sofia, Bulgaria
christov_ivan@abv.bg

Radoslava Hristova
Faculty of Mathematics and Informatics
St. Kliment Ohridski University of Sofia
5 James Bourchier Blvd
1164 Sofia, Bulgaria
radoslava@fmi.uni-sofia.bg

Dimitar Iankov
Fraunhofer Institute for Applied Solid State Physics IAF
Tullastrasse 72
79108 Freiburg
dimitre.iankov@iaf-extern.fraunhofer.de

Roumen Iankov
Institute of Mechanics
Bulgarian Academy of Sciences
Acad. G. Bontchev St., bl. 4
1113 Sofia, Bulgaria
iankovr@yahoo.com

Rossen Ivanov
School of Mathematical Sciences
Dublin Institute of Technology
Kevin Street, Dublin 8
IRELAND
rossen.ivanov@dit.ie

Tihomir Ivanov
Institute of Mathematics and Informatics
Bulgarian Academy of Sciences
Acad. G. Bontchev str., bl. 8
1113 Sofia, Bulgaria;
Faculty of Mathematics and Informatics,
Sofia University
5 James Bourchier
1164 Sofia, Bulgaria
tbivanov@fmi.uni-sofia.bg

Yonka Ivanova
Faculty of Physics
Sofia University "St. Kliment Ohridski"
Blvd. James Bourchier 5
1164 Sofia, Bulgaria
yonivan@phys.uni-sofia.bg
and
Institute of Mechanics
Bulgarian Academy of Sciences
Acad. G. Bonchev Str., Bl. 4,
1113 Sofia, Bulgaria
yonka@imbm.bas.bg

Stanimir Kabaivanov
Plovdiv University
"Tzar Assen" str. 24
Plovdiv, Bulgaria
stanimir.kabaivanov@gmail.com

Aneta Karaivanova
Institute of Information and Communication Technologies
Bulgarian Academy of Sciences
Acad. G. Bontchev str., bl. 25A
1113 Sofia, Bulgaria
anet@parallel.bas.bg

Tzanio Kolev
Lawrence Livermore National Laboratory
7000 East Avenue
94550 Livermore, CA, USA
kolev1@llnl.gov

Hristo Kostadinov
Institute of Mathematics and Informatics
Bulgarian Academy of Sciences
Acad. G. Bonchev St., Bl.8
1113 Sofia, Bulgaria
hristo@math.bas.bg

Liliya Kraleva
Institute of Mathematics and Informatics
Bulgarian Academy of Sciences
Acad. G. Bonchev St., Bl.8
1113 Sofia, Bulgaria

Johannes Kraus
University of Duisburg-Essen
Thea-Leymann-Str. 9
45127 Essen, Germany
johannes.kraus@uni-due.de

William Lee
MACSI
Department of Mathematics and Statistics
University of Limerick
Limerick, Ireland
william.lee@ul.ie

Konstantinos Liolios
Institute of Information and
Communication Technologies
Bulgarian Academy of Sciences
Acad. G. Bontchev str., bl. 25A
1113 Sofia, Bulgaria
kliolios@parallel.bas.bg

Nikolai Manev
USEA (VSU) "Lyuben Karavelov"
Suhodolska Str., 175
1373 Sofia, Bulgaria
and
Institute of Mathematics and Informatics
Bulgarian Academy of Sciences
Acad. G. Bonchev St., Bl.8
1113 Sofia, Bulgaria
nlmanev@math.bas.bg

Angel Marchev, Jr.
University of National and
World Economy
Students Town
1700 Sofia, Bulgaria
angel_marchev@yahoo.co.uk

Svetozar Margenov
Institute of Information and
Communication Technologies
Bulgarian Academy of Sciences
Acad. G. Bonchev Str., bl. 25A
1113 Sofia, Bulgaria
margenov@parallel.bas.bg

Lubomir Markov
Department of Mathematics and CS
Barry University
11300 N.E. Second Avenue
Miami Shores, FL 33161, USA
lmarkov@barry.edu

Mariyan Milev
University of Food Technologies
26 Maritsa Blvd.
4000 Plovdiv, Bulgaria
m_milev@uft-plovdiv.bg

Ivaïlo M. Mladenov
Institute of Biophysics
Bulgarian Academy of Sciences
Acad. G. Bonchev Str., Bl. 21
1113 Sofia, Bulgaria
mladenov@bio21.bas.bg

Clementina D. Mladenova
Institute of Mechanics
Bulgarian Academy of Sciences
Acad. G. Bonchev Str., Bl. 4,
1113 Sofia, Bulgaria
clem@imbm.bas.bg

Maya Neytcheva
Department of Information Technology
Uppsala University
Box 337
75105 Uppsala, Sweden
maya.neytcheva@it.uu.se

Nikola Nikolov
Institute of Mechanics
Bulgarian Academy of Sciences
Acad. G. Bontchev str., bl. 4
1113 Sofia, Bulgaria
n.nikolov@imbm.bas.bg

Elena Nikolova
Institute of Mechanics
Bulgarian Academy of Sciences
Acad. G. Bontchev str., bl. 4
1113 Sofia, Bulgaria
elena@imbm.bas.bg

Silviya Nikolova
Department of Anthropology
and Anatomy
Institute of Experimental Morphology,
Pathology and Anthropology
with Museum
Bulgarian Academy of Sciences
Acad. G. Bonchev Str., bl. 25
1113 Sofia, Bulgaria
sil_nikolova@abv.bg

Todor Partalin
Faculty of Mathematics and Informatics
Sofia University "St. Kliment Ohridski"
Blvd. James Bourchier 5
1164 Sofia, Bulgaria
topart@fmi.uni-sofia.bg

Tania Pencheva
Institute of Biophysics and
Biomedical Engineering
Bulgarian Academy of Sciences
105 Acad G. Bonchev Str.
1113 Sofia, Bulgaria
tania.pencheva@biomed.bas.bg

Evgenija D. Popova
Institute of Mathematics and Informatics
Bulgarian Academy of Sciences
Acad. G. Bonchev str., block 8
1113 Sofia, Bulgaria
epopova@math.bas.bg
epopova@bio.bas.bg

Stefan Radev
Institute of Mechanics
Bulgarian Academy of Sciences
Acad. G. Bontchev str., bl. 4
1113 Sofia, Bulgaria
stradev@imbm.bas.bg

Plamen Rajnov
University of Food Technologies
26 Maritsa Blvd.
4000 Plovdiv, Bulgaria
plamsky@mail.bg

Peter Rashkov
Biosciences, College of Life and
Environmental Sciences
University of Exeter
Exeter EX44QD, UNITED KINGDOM
p.rashkov@exeter.ac.uk

Olympia Roeva
Institute of Biophysics and
Biomedical Engineering
Bulgarian Academy of Sciences
Acad. G. Bontchev str., bl. 105
1113 Sofia, Bulgaria
olympia@biomed.bas.bg

Sonia Tabakova
Institute of Mechanics,
Bulgarian Academy of Sciences
Acad. G. Bontchev str., bl. 4
1113 Sofia, Bulgaria
Technical University - Sofia,
Branch Plovdiv
25 Tzanko Djustabanov str.
4000 Plovdiv, Bulgaria
stabakova@gmail.com

Assen Tchorbadjieff
Institute of Mathematics and Informatics
Bulgarian Academy of Sciences
Acad. G. Bonchev Str., Bl. 8
1113 Sofia, Bulgaria
tchorbadjieff@hotmail.com

Margarita Terziyska
Institute of Information and
Communication Technologies
Bulgarian Academy of Sciences
Acad. G. Bontchev str., bl. 2
1113 Sofia, Bulgaria
mterziyska@bas.bg

Yancho Todorov
Institute of Information and
Communication Technologies
Bulgarian Academy of Sciences
Acad. G. Bontchev str., bl. 2
1113 Sofia, Bulgaria
yancho.todorov@iit.bas.bg

Diana Toneva
Department of Anthropology
and Anatomy
Institute of Experimental Morphology,
Pathology and Anthropology
with Museum
Bulgarian Academy of Sciences
Acad. G. Bonchev Str., bl. 25
1113 Sofia, Bulgaria
ditoneva@abv.bg

Vassilios Tsihrintzis
Centre for the Assessment of
Natural Hazards and Proactive Planning,
and
Laboratory of Reclamation Works and
Water Resources Management
Department of Infrastructure and
Rural Development
School of Rural and
Surveying Engineering
National Technical University of Athens
9 Iroon Polytechniou St.,
Zografou, 157 73 Athens, Greece
tsihrin@central.ntua.gr

Daniela Vasileva
Institute of Mathematics and Informatics
Bulgarian Academy of Sciences
Acad. G. Bonchev Str., Bl. 8
1113 Sofia, Bulgaria
vasileva@math.bas.bg

Vladimir Veliov
Institute of Statistics and Mathematical
Methods in Economics
Vienna University of Technology
Wiedner Hauptstrasse 8/ E105-4
1040 Vienna, Austria
veliov@tuwien.ac.at

Milena Veneva
Faculty of Mathematics and Informatics
Sofia University "St. Kliment Ohridski"
5 James Bourchier blvd.
1164 Sofia, Bulgaria
milena.p.veneva@gmail.com

Krassimira Vlachkova
Faculty of Mathematics and Informatics
Sofia University "St. Kliment Ohridski"
Blvd. James Bourchier 5
1164 Sofia, Bulgaria
krassivl@fmi.uni-sofia.bg

Yavor Vutov
Institute of Information and
Communication Technologies
Bulgarian Academy of Sciences
Acad. G. Bonchev Str., bl. 25A
1113 Sofia, Bulgaria
yavor@parallel.bas.bg

Alexandar B Yanovski
Department of Mathematics and
Applied Mathematics
University of Cape Town
Rondebosch 7701, South Africa
alexandar.ianovsky@uct.ac.za

Roussislava Zaharieva
Institute of Mechanics
Bulgarian Academy of Sciences
Acad. G. Bontchev St., bl. 4
1113 Sofia, Bulgaria
rusislava@ imbm.bas.bg

Ludmil Zikatanov
Penn State University
311 McAllister Bldg
16802 University Park, PA, USA
ltz@math.psu.edu
and
Institute of Mathematics and Informatics
Bulgarian Academy of Sciences
Acad. G. Bonchev Str., Bl. 8
1113 Sofia, Bulgaria